T.C
ISTANBUL UNIVERSITY-
CERRAHPASA
INSTITUTE OF GRADUATE

VANADIUM REMOVAL FROM AQUEOUS SOLUTIONS BY AMINO-FUNCTIONALIZED POLYMER IN FIXED-BED COLUMN

M.Sc. THESIS

Abdoulaye Mamadou TRAORE

Environmental Engineering Department

Supervisor

Assoc. Prof. Serdar AYDIN

Department of Environmental Engineering

Environmental Engineering Programme

ISTANBUL July, 2019

This study was accepted on 26/7/2019 as a M. Sc. thesis in Department of Environmental Engineering, Environmental Engineering Programme by the following Committee.

Examining Committee Members

Assoc. Prof. Dr. Serdar AYDIN(Supervisor)
İstanbul University-Cerrahpaşa
Faculty of Engineering

Assoc. Prof. Dr. Serkan EMIK
İstanbul University-Cerrahpaşa
Faculty of Engineering

Dr. Öğr. Üyesi Ayça BAL ÖZTÜRK
Istinye University
Faculty of Engineering

As required by the 9/2 and 22/2 articles of the Graduate Education Regulation which was published in the Official Gazette on 20.04.2016, this graduate thesis is reported as in accordance with criteria determined by the Institute of Graduate Studies by using the plagiarism software to which Istanbul University-Cerrahpasa is a subscriber.

This thesis is supported by the project numbered..... of Istanbul University-Cerrahpaşa Scientific Research Projects Executive Secretariat.

This thesis is supported by the project numbered ..... of .....

FORWARD

I would like to thank my family Senior Colonel Adama TRAORE and Mrs. TRAORE Badiallo for their unconditional love and support they have given me all the way through my life, education and career. I would like to also thank to my supervisors, Assoc. Prof. Serdar AYDIN and Assoc. Prof. Serkan EMIK for the guidance and counsel they have given me as well as the patience and compassion they have shown towards me since the beginning of this project. I also acknowledge the encouragement to give my best and support received from my amazing wife Mrs.TRAORE Samira and my untiring father Senior Colonel Adama TRAORE. Finally I am grateful to God for blessing me with this amazing love and support system.

July, 2019 **Abdoulaye Mamadou TRAORE**

TABLE OF CONTENTS

TABLE OF CONTENTS v
LIST OF FIGURES vii
LIST OF TABLES ix
ABSTRACT x
1 INTRODUCTION 1
1.1 Problem statement 3
1.1.1 Purpose of the Study 3
1.1.2 Objectives 3
2 LITERATURE REVIEW 4
2.1 WASTEWATER TREATMENT METHODS 4
2.1.1 Physical Method 4
2.1.2 Biological Method 4
2.1.3 Chemical Method 5
2.1.4 Coagulation-flocculation 5
2.1.5 Precipitation 6
2.1.6 Ion exchange 7
2.1.7 Irradiation 8
2.2 OTHER METHODS 8
2.2.1 Reverse Osmosis / Membrane 8
2.2.2 Distillation / Thermal 9
2.2.3 Adsorption 9
2.3 ADSORBENTS 9
2.3.1 Coal waste 9
2.3.2 Magnetized Adsorbents 10
2.3.3 Polymeric Adsorbents 11
2.3.4 Conducting Polymers 11
2.4 VANADIUM 12
2.4.1 Vanadium Sources 12
2.4.2 Uses of Vanadium 12
2.4.3 Health Impact of Vanadium 13

2.5 MATHEMATICAL DESCRIPTION 13
2.5.1 Thomas model 14
2.5.2 Adams–Bohart model 15
2.5.3 Yoon–Nelson model 15
2.5.4 Clark model 15
2.5.5 Bed-depth or service time analysis (BDST) model 16
3 MATERIALS AND METHODS 18
3.1 CHEMICALS 18
3.2 GENERAL ADSORPTION STUDIES AND PROCEDURE 18
4 RESULTS AND DISCUSSION 21
4.1 EFFECTS ON THE BREAKTHROUGH CURVE 21
4.1.1 Effect of the flow rate on the breakthrough curve 21
4.1.2 Effect of the concentration on the breakthrough curve 21
4.1.3 Effect of different bed depth on the breakthrough curve 22
4.2 DISCUSSION 24
4.2.1 Thomas model 24
4.2.2 Yoon–Nelson model 35
4.2.3 Bed Depth-Time Service (BDST) Model 46
5 CONCLUSION 50
6 REFERENCES 51
7 APPENDICES 55
7.1 Appendix 1: Experimental data first group of experiments effect of concentration on the breakthrough curve 55
7.2 Appendix 2: Experimental data second group of experiments effect of the flow rate on the breakthrough curve 60
7.3 Appendix 3: Experimental data third group of experiments effect of different bed depth on the breakthrough curve 65
CURRICULUM VITAE 71

LIST OF FIGURES

Page

Figure 1: fixed bed column adsorber……21

Figure 2: Calibration line ……....21

Figure 3: Breakthrough curves: the effect of flow rate on Vanadium……..…...23

Figure 4: Breakthrough curves: the effect of influent concentration on Vanadium……..…...24

Figure 5: Breakthrough curves: the effect of different bed depths on Vanadium adsorption..25

Figure 6: Thomas model graph K_{th} and q_o values at 100 ppm...……..28

Figure 7: Comparison of experimental values to theoretical values Thomas model……28

Figure 8: Thomas model graph K_{th} and q_o values at 50 ppm…….29

Figure 9: Comparison of experimental values to theoretical values Thomas model……29

Figure 10: Thomas model graph K_{th} and q_o values at 75 ppm….……....30

Figure 11: Comparison of experimental values to theoretical values Thomas model…..……30

Figure 12: Thomas model graph K_{th} and q_o values at Q=7.5ml/min.....……...31

Figure 13: Comparison of experimental values to theoretical values Thomas model…….31

Figure 14: Thomas model graph K_{th} and q_o values at Q= 10 ml/min.....…….....32

Figure 15: Comparison of experimental values to theoretical values Thomas model…….32

Figure 16: Thomas model graph K_{th} and q_o values at Q=12.5ml/min.....…….……33

Figure 17: Comparison of experimental values to theoretical values Thomas model…….33

Figure 18: Thomas model graph K_{th} and q_o values at Z= 2 cm …….....…….……34

Figure 19: Comparison of experimental values to theoretical values Thomas model…….34

Figure 20: Thomas model graph K_{th} and q_o values at Z= 3 cm …….....…….……35

Figure 21: Comparison of experimental values to theoretical values Thomas model…….35

Figure 22: Thomas model graph K_{th} and q_o values at Z= 4 cm …….....…….……36

Figure 23: Comparison of experimental values to theoretical values Thomas model…..…..36

Figure 24: Yoon-Nelson model graph K_{YN} and τ values at 100 ppm …….....…….……...39

Figure 25: Comparison of experimental values to theoretical values Yoon-Nelson model….39

Figure 26: Yoon-Nelson model graph K_{YN} and τ values at 50 ppm ...…….....…….……..40

Figure 27: Comparison of experimental values to theoretical values Yoon-Nelson model….40

Figure 28: Yoon-Nelson model graph K_{YN} and τ values at 75 ppm ...…….....…….……..41

Figure 29: Comparison of experimental values to theoretical values Yoon-Nelson model….41

Figure 30: Yoon-Nelson model graph K_{YN} and τ values at Q = 7.5 ml/min.....…….……..42

Figure 31: Comparison of experimental values to theoretical values Yoon-Nelson model….42

Figure 32: Yoon-Nelson model graph K_{YN} and τ values at Q = 10 ml/min.....…….……..43

Figure 33: Comparison of experimental values to theoretical values Yoon-Nelson model….43

Figure 34: Yoon-Nelson model graph K_{YN} and τ values at Q =12.5 ml/min.....……..44

Figure 35: Comparison of experimental values to theoretical values Yoon-Nelson model….44

Figure 36: Yoon-Nelson model graph K_{YN} and τ values at Z = 3 cm…….....……..45

Figure 37: Comparison of experimental values to theoretical values Yoon-Nelson model….45

Figure 38: Yoon-Nelson model graph K_{YN} and τ values at Z = 2 cm…….....……..46

Figure 39: Comparison of experimental values to theoretical values Yoon-Nelson model….46

Figure 40: Yoon-Nelson model graph K_{YN} and τ values at Z = 4 cm…….....……..47

Figure 41: Comparison of experimental values to theoretical values Yoon-Nelson model….47

Figure 42: BDST model graph K_o and N_o values at 2; 3 and 4 cm ...…….....……..50

Figure 43: Comparison of experimental to theoretical values BDST model at 100ppm…….51

Figure 44: Comparison of experimental to theoretical values BDST model at 75ppm…..….51

Figure 45: Comparison of experimental to theoretical values BDST model at 50ppm…..….52

LIST OF TABLES

Page

Table 1: Parameters of Thomas model ……35

Table 2: Parameters of Yoon-Nelson model……46

Table 3: Parameters of BDST model……....49

ABSTRACT

MSc. THESIS

REMOVAL FROM AQUEOUS SOLUTIONS BY AMINO-FUNCTIONALIZED POLYMER IN FIXED-BED COLUMN

Abdoulaye Mamadou TRAORE

Istanbul University

Institute of Science

Department of Environment Engineering

Supervisor: Assoc. Prof. Serdar AYDIN

Medium-hard, steel-blue Vanadium is a metal. Although not a much known metal, vanadium is highly valuable in the manufacturing industry since its malleable, ductile and corrosion-resistant qualities. In this study, vanadium removal studies were carried out in fixed bed column of an amino functional polymeric adsorbent. For this purpose, in the scale of a laboratory fixed bed column, vanadium removal was investigated in a continuous system and the effects of the initial concentration, bed depth and feed flow rate on the adsorption process were examined. The Thomas and BDST models (Bed Depth Service Time) equations were used on the experimental results and the column bed performances were examined .The Langmuir adsorption capacity at 25 ^{0}C and pH 4.5 is 65.36 mg/L for vanadium. Vanadium adsorption is temperature dependent (endothermic) and spontaneous attaining equilibrium within 30 minutes.

July, 2019: 81 Pages

Keywords: Bed Depth Service Time; Conducting Polymers; waste water treatment; fixed bed column

1 INTRODUCTION

Vanadium is a rare earth element that has been used extensively as an alloy in steel, jet and high-speed aircraft manufacturing (Gasik, 2013; Kajjumba et al., 2017). In addition, vanadium is used in superconducting magnetic and as a catalyst in production of sulphuric acid. And recently, vanadium has been reported to be a high energy storage material (Evans et al., 2012). With all these developments, vanadium concentration in water is on increase. On health side, when vanadium is applied in the right quantities, it has been reported to slow down the formation of cholesterol in the blood, prevent heart disease and tooth decay (Mazed and Mazed, 2010). However, elevated concentration of vanadium consumption has been linked to manic depression-a condition that can cause serious shifts in mood, thinking behaviour, energy, and excess mucus production (Assem and Oskarsson, 2015). Common anions associated with vanadium include sulphate and chloride ions. Such compounds when consumed cause dermatitis, flushing, hypotension, abdominal pain, eutrophication (Assem and Oskarsson, 2015; Mazed and Mazed, 2010; Smolders et al., 2010). It is, therefore, important to treat vanadium salt polluted wastewater before it is dumped into any water body.

A compound can be separated from Wastewater if it is selectively adsorbed on top of a solid surface. This process is called adsorption. Adsorbents are most of the time porous solids but they can also be liquids such as silica gel which adsorbs moisture, activated carbon which adsorbs organic matters, zeolites, molecular sieves and synthetic resins.

A wide variety of physical, chemical and biological techniques have been developed and tested in the treatment of wastewater. These processes include coagulation-flocculation, precipitation, ion exchange, membrane filtration, irradiation and ozonation. However, these methods are expensive and lead to the generation of large quantities of sludge or the formation of

derivatives. Among the liquid discharge treatment processes, adsorption remains a relatively used and easy to implement technique.

Activated carbon is the most widely used adsorbent because of its high adsorption capacity of organic materials. However, this adsorbent has a high cost and remains difficult to regenerate. The search for another effective and less expensive adsorbent is therefore interesting. In this context, the use of polymers as adsorbent is of great interest because of its efficiency, affordability.

Synthesizing the specific polymeric adsorbent with the specific functional groups that affects the effectiveness, capacity, selectivity and reusability of the adsorbent is like making the perfect key to a specific lock for researchers. To remove heavy metals like vanadium from wastewater amino fictionalized groups have been one the most effective adsorbents. Interpenetrating polymer networks (IPNs) are one the best polymeric adsorbents due their composition. They are made by a mixture of two intertwined polymers with entangled networks, the hydrogel based IPNs have strength due to their entangled structure.

Poly (glycidyl methacrylate) (pGMA) is a polymer matrix that has resistance to acids and alkali and also has a strong and porous structure.

IPNs that are that made of pGMA and poly (amino acids) pAA could be great polymeric absorbents, but can they be used as adsorbents for a vanadium adsorption.

1.1 Problem statement

Heavy metals removal from wastewater has received considerable attention while little has been given to rare metals like vanadium. One of the commonest form of vanadium in wastewater is $VOSO_4$. With the recent development in nanomaterial, adsorption has become a competitive mechanism to remove wastes from solution. The choice of an adsorbent depends on availability, cost and efficiency. Conducting Polymers has been reported to be a good adsorbent of wastes from wastewater, however for effective adsorption, an investigation is necessary using conducting polymers (polyaniline) can offer good results.

1.1.1 Purpose of the Study

In this study, vanadium removal studies were carried out in fixed bed column of an amino functional polymeric adsorbent to investigate vanadium removal in a continuous system, examine the effects of bed height and feed flow rate on the adsorption process and the initial concentration.

1.1.2 Objectives

a. To investigate vanadium removal in a continuous system and examine the effects of bed height and feed flow rate on the adsorption process and the initial concentration.

2 LITERATURE REVIEW

2.1 WASTEWATER TREATMENT METHODS

When organic and inorganic matters are discharged into the water body, the levels of dissolved oxygen are affected. Organic matter consume oxygen resulting in oxygen deficiency, while nutrients (phosphates and nitrates) promote the growth of algae and plankton (Bock et al., 2015), this affects the eco-system in the water bodies. In addition, some of the organic and inorganic materials discharged are dangerous to human when consumed. Thus, a need for treatment of wastewater before it is discharged into the receiving water body. A number of processes have evolved in the past decades.

2.1.1 Physical Method

Physical (mechanical) treatment approach uses sedimentation technique to remove large particles from wastewater. It is estimated that only a third of the waste can be removed using this approach (Kurniawan et al., 2006). Therefore, mechanical treatment method must be supplemented with biological or chemical or both to meet the stringent levels of effluent water.

2.1.2 Biological Method

The biological treatment uses microorganism that feeds on the substrate in the wastewater. As these microorganisms feed on the substrate, they grow and the excess is separated as sludge. Biological treatment method has a capacity to remove both solid and dissolved organic matter (Fakhru'l-Razi et al., 2009; Türgay et al., 2011). The choice of any treatment method depends on efficiency, cost, byproduct handling and how fast it takes to treat the wastewater. Biological method, a huge amount of air and land are required to operate the system. The process of blowing in the air makes the construction and operation of biological plants a complex (Hosomi, 2016).

2.1.3 Chemical Method

Chemical treatment uses coagulants (alum and ferric) to precipitate the organic and inorganic waste that are separated as sludge. The chemical method takes less time compared to biological for a given volume of wastewater because, for biological process, microorganisms have to adapt to influent wastewater (Bratby, 2016; Kurniawan et al., 2006; Song et al., 2015). With chemical process, little amount coagulant is mixed with influent in a small poll at low energy consumption.

2.1.4 Coagulation-flocculation

Coagulation-flocculation is a physio-chemical process that makes the agglomeration of fine particles (colloids) in water to form a floc which can easily be filtered from water. Effluents (wastewater) have to be treated before being discharged or reused. The coagulation-flocculation contributes to the elimination of the effluent compounds and thus allows a separation of water and particles. The use of COAGULANTS and FLOCCULANTS is necessary for your paint booths, robots and water curtain tunnels to stay clean and operate as efficiently as possible. Coagulants, liquid products used primarily for the treatment of circulating water in paint booths. The addition of a coagulant reagent to wastewater makes it possible to destabilize the colloidal particles suspended in water. Indeed, the purpose of the coagulant is to reduce or even neutralize the negative electric charge of the colloid to promote their approximation. The particles will agglomerate and form what are called "flocs". However, these flocs remain fragile and small; the addition of a flocculent is therefore necessary. However flocculants, liquid products that facilitate contact between previously destabilized particles, unloaded by coagulation. The agitation of the fluid causes the agglomeration of the pigments. This reaction allows a magnification of the flocs which will facilitate and improve

the solid-liquid separation, separation which will be ensured by decantation or flotation. However this water treatment method has a high cost.

2.1.5 Precipitation

In water treatment, chemical precipitation (excluding coagulation-flocculation) is mainly used to eliminate by insolubilization one or more mineral compounds that hinder the use of water, among others: hardness (Ca^{2+} and Mg^{2+}), metals, some anions such as SO_4^{2-}, PO_4^{3-}, F^- ...

It will therefore be sought in each case to bring to the water in the form of soluble reagent, the ion making it possible to form, with the annoying compound, a precipitate as little soluble as possible. At given temperature and pH, the residual solubility is governed by the solubility product (Ks) of the precipitating body. This allows the need to adjust the residual value of the annoying ion by shifting the equilibrium by overdosing (exceeding the stoichiometric dose) the reagent. In the case of Ca and Mg, it is not only these ions that can be troublesome (overconsumption of detergents or taste of water ...) but especially the precipitation of calcium carbonate (scaling); it is therefore firstly the precipitation potential (produces concentrations of Ca and CO_3) which is decisive. Moreover, Ca and Mg are rather favorable for human health and are only troublesome at very high levels or for cleaning applications. The terms used traditionally are often unsuited to the reality of the phenomenon when "softening" and "decarbonation" are the two facets of calcium carbonate precipitation. On the other hand one can "soften" with resins or "decarbonate" by degassing CO_2, two phenomena far from chemical precipitation. This practice is nevertheless expensive (high consumption of reagents) and leaves in the treated water the excess of reactive ion which, in certain cases, can itself become annoying.

2.1.6 Ion exchange

Insoluble granular substances, Ion exchangers having in their molecular structure radicals that are acidic or basic capable of permuting, without any apparent modification of their appearance, and without alteration or solubilization, the negative or positive ions, "fixed" on these radicals, against same sign ions found in solution in the liquid at their contact. This permutation called ion exchange makes it possible to modify the ionic composition of the liquid that is the subject of the treatment, without modifying the total number of charges existing in this liquid before the exchange. The ion exchangers were first natural earth (zeolites), then synthetic mineral compounds (silicoaluminates) then organic, the latter being almost exclusively used today as resins. They are either in the form of grains or, for the majority of them, in the form of beads. We distinguish the skeleton of the resin and the active sites grafted on this skeleton. Currently, three types of skeleton exist industrially: polystyrene, acrylic and formophenolic. The first two result from a polymerization (with formation of beads), the last of a condensation (with formation of grains). The polymerized skeletons are cross-linked by an agent such as divinylbenzene. A high degree of crosslinking increases the resistance to both mechanical stresses (pressure drops) and osmotic stresses (related to ionic change). The gel type resins have a homogeneous structure. The macroporous backbone resins comprise a porosity obtained by the addition of a pore-forming solvent. The macropores obtained create a discontinuity in the crystalline structure that becomes opaque to light. Macroporous resins are highly cross-linked and have a better adsorption and desorption capacity of organic materials. The cationic or anionic active sites are then grafted onto the backbone to give acids or bases, their strength depends on the fixed radical (HCO_2^-, HSO_3^-, NH_3^+, etc.). By convention, a resin having anionic grafted active sites is called a cationic resin since it will make it possible to exchange the cations ... and vice versa and this R-Ca or R-Na resin is noted according to

whether it is charged with ions. Ca^{2+} or Na^{+}. This system requires a high amount of energy and is costly.

2.1.7 Irradiation

This treatment method uses the bactericidal treatment device that has the principle of generating ultraviolet rays within a chamber of irradiation. These rays irradiate the living cells which are in the liquid going through the apparatus. The basic principle, known since the beginning of the century, today benefits from new materials (high germicidal lamps, and irradiation chamber with high reflection coefficient), and a total control of the ancillary parameters of operation (environment, flow, application). Since the quality of water has been pointed out for a few years now, the principle of UV decontamination has developed a lot. The sterilizing action is a result of the disturbance of the ultra-violet radiations in the chemical structure of the contents of the living cell, and consequently, of their operation. The adsorption curve of DNA (deoxyribonucleic acid), a real support for genetic information in the nucleus of cells, for wavelengths between 200 and 285 nm shows a peak at the wavelength 257 nm, i.e. a deep germicidal effect at this wavelength. But the effectiveness of the treatment cannot be appreciated immediately by measuring residues, there is no residual effect and finally using UV disinfection is only for the disinfection of waters that have distribution short and well maintained circuit.

2.2 OTHER METHODS

2.2.1 Reverse Osmosis / Membrane

A water treatment process, reverse osmosis is a process that abstracts contaminants from wastewater by utilizing pressure to push water through a semipermeable membrane. In this process, the contaminants are filtered and flushed leaving clean drinking water (Nataraj et al., 2006). Reverse osmosis can remove contaminants and recovery of metals including lead,

fluoride, chloride, colour, organic contaminants, nitrate and dissolved salts from the feed stream (Garud et al., 2011). As investigated by (Chen et al., 2016), at 55^0C reverse osmosis leads to higher silica and boron recovery. Furthermore, the investigation of forward osmosis (Ortega-Bravo et al., 2016), revealed a promising method of treating wastewater but the process needs low water-flux. The main fiasco of reverse osmosis in desalination is membrane biofouling and high amount of energy required to run the system.

2.2.2 Distillation / Thermal

This process of water desalination involves boiling the water and then condensing the steam into clean containers. This process of water purification has been in use since 200 AD. The debacle associated with this method is the high energy requirements, scaling and also requires a large operating area for the huge amount of water (Paraskeva and Diamadopoulos, 2006).

2.2.3 Adsorption

Adsorption is the penetration of atoms (adsorbate) onto the solid surface (adsorbent) by creating a film around. Depending on the surface characteristics of the adsorbent, adsorption can be classified as chemisorption or physisorption. Physical adsorption is governed by Vander Waal's forces—which are weak; therefore, increase in temperature or decreasing pressure can reverse the process (Hu et al., 2014). Chemical adsorption is a result of the chemical bond between adsorbate and adsorbent.

2.3 ADSORBENTS

2.3.1 Coal waste

Coal processing and production give a vast amount of wastes , its consumption is expected to increase (Höök et al., 2010). In 2014, the consumption of coal was between 5 – 6 Gt worldwide (United Nations, 2016) of which 10 – 15% is coal waste (Haibin and Zhenling, 2010). Coal

wastes constitute of illite and quartz when unburnt, but those burnt contain illite, quartz, mullite, jarosite and a high amount of amorphous material (Ribeiro et al., 2010). Coal has been recycled in different forms including Coal ash which can act as a bidder material in construction and also ceramic and glass production (Haibin and Zhenling, 2010), soil betterment as a result of its buffering characteristics (Blissett and Rowson, 2012). With modification, coal has been used as an adsorbent (Mohan and Gandhimathi, 2009). Tons of unburnt coal waste are thrown off in landfills (Haibin and Zhenling, 2010). Presence of high content of carbon makes coal waste a fairly good adsorbent material; however, separation of coal waste after adsorption is a problem. Also, to achieve maximum adsorption capacity of unburnt coal waste, modifications are necessary.

2.3.2 Magnetized Adsorbents

Magnetic related materials have been employed in water treatment since late 19th century. Since then, magnetic materials have been used in coagulation, anti-scaling of pipelines, biological processes (Ambashta and Sillanpää, 2010; Narayanan and Sakthivel, 2010). However, their application in adsorption mechanism is a new concept. Generally, in adsorption, the magnetic material like Fe, Co, Ni and Cu is impregnated into the base adsorbent. The main purpose of embedding these elements is to ease separation upon application of an external magnet (Mthombeni et al., 2016). To make the adsorption better and to improve stability of magnetic adsorbents, they have been modified with polymers.

2.3.3 Polymeric Adsorbents

Polymeric adsorbents are sphere shaped synthetic polymers that are used for the removal of organic molecules in aqueous solution. The range of application is quite vast from removal of protein in lysed cells to removal of metals in wastewater. Making specific polymeric absorbents that have significant effects on the effectiveness, the capacity, the selectivity and reusability is the biggest problem a researcher faces. But their throughout researches, they have found that the carboxyl and amine groups are the most suitable functional groups. In comparison with other regular polymeric absorbents recently interpenetrating polymer networks (IPNs) have gained more attention, because they are mostly a mixture of at least two cross linked polymers (Serkan Emik et al.2014). Poly (glycidyl methacrylate) (pGMA), one of the highly studied polymer matrix a result of its good mechanical strength, its resistance to acid and alkali, its porous structure and its cheaper cost compared to any other vinyl polymers with high reactive epoxy groups in the side chain (Serkan Emik et al.2014).

2.3.4 Conducting Polymers

In the recent years, conducting polymers have received great attention in wastewater treatment. This is attributed to the fact that they can improve mechanical, thermal chemical and physical properties of a base adsorbent making it suitable for the adsorption process (Bolan et al., 2013). In addition, when merged together with the adsorbent, they improve the surface area of the composite (Mthombeni et al., 2016). Conducting polymers exhibit high boiling temperature due to lack of free rotating groups and full aromatic ring (Das and Prusty, 2012). Some of the major conduction polymers include; polyacetylene, polyphenylene, polypyrrole, polythiophene, and polyaniline. In addition, polypyrrole and polyaniline have produced promising results in adsorption technology. Polyaniline has an amine group in the major skeleton. Its production is easy, moderately inexpensive, and can be chemically modified with ease (Suckeveriene et al., 2011).

2.4 VANADIUM

Vanadium, a rare metal (0.01% of the earth's crust) with a silver color. It can be in different forms of oxides and complexes (-1, 0, +2, +3, +4, +5). Vanadium pentoxide is the most stable of its state (Kajjumba et al., 2017).

2.4.1 Vanadium Sources

Except its own ores, vanadium oxides are taken from iron ores and uranium ores and the salt roast process. The environmental contamination by vanadium is a result of combustion of fuels (Gasik, 2013). Estimations are that 69,000 tons of vanadium are released into the atmosphere annually (United Nations, 2016). Mostly concentrations of vanadium in coal go from 14-56 mg/Kg (Zhang et al., 2011). When burnt, vanadium remains solid, soot, fly ash and boiler scale as vanadium pentoxide. Vanadium is utilised in power grid systems to be an energy storage material (Dunn et al., 2011). The consumption of fuels and the development of energy storage systems is increasing and the pollution levels of vanadium are also going to increase. Water bodies and the soil pollution can easily happen if vanadium sediments are subjected to acidic conditions (pH$\leq$ 2) (Zhang et al., 2011).

2.4.2 Uses of Vanadium

Globally, 85% of the produced vanadium is used in steel industry where it is used as an alloy; 10% is in titanium sectors, and 5% is used in others sectors like aerospace and medicine (Gasik, 2013). As an alloy of steel, it is used as ferrovanadium that is used in crankshaft and gears because of its excellent properties of corrosion and shock resistance. As a titanium alloy, it is used in high-speed aircraft and in jet engines. Vanadium is used in the formation of vanadium-gallium a superconducting magnet (Zhang et al., 2011). Vanadium has been also employed as a catalyst in a number of reactions—for example in the production of sulphuric acid. Because

of its resistance to neutron adsorption, vanadium is employed in nuclear plants. Vanadium as vanadium pentoxide is used to permanently fix dye in fabrics (Rauf et al., 2011).

2.4.3 Health Impact of Vanadium

Currently, vanadium is used in diabetes, heart, tuberculosis, low sugar level treatment. Also, it is used in the reduction of cholesterol levels and improvement of water retention for athletics (Mazed and Mazed, 2010). In animal cells, vanadium is a great stimulus of vascular permeability factor which is reason for the creation of new or rebuilding lesion blood vessels (Mazed and Mazed, 2010). But, vanadium has a lot of effects in mammals and birds. For instance, high concentrations of vanadium (5‑10 mg/kg) lowers egg albumen quality (Yuan et al., 2016). Vanadium compounds (sodium metavanadate) at high levels make epididymis weight loss, sperm count lowered in males, chronic inflammations of the trachea, eye soar and high neoplastic cell growth. Vanadium is a strong inhibitor of phosphatases as other oxoanions in ribonuclease (Zhang et al., 2011).

2.5 MATHEMATICAL DESCRIPTION

The behaviour of a fixed-bed column is best described with the concept of the breakthrough curve. Breakthrough appearance time and the shape of the breakthrough curve are the most important characteristics to find the operation and the dynamic response of an adsorption column. The loading behavior of Vanadium to be adsorbed from liquid waste in a fixed-bed is most of the time expressed as Ct /Co as a function of time or volume of the out-flow for a given bed depth, giving a breakthrough curve (Z.Aksu et al., 2004). The value of q_{total} for a given feed and flow is the area under the plot of the removed vanadium concentration C_{ad} ($C_{ad} = C_0 - C_t$) (mg l^{-1}) vs. t (min) and can be found from Equation 1:

$$q_{total} = \frac{Q}{1000} \int_{t=0}^{t=t_{total}} c_{ad}\, dt \qquad (1)$$

The value of $q_{e(exp)}$ is calculated at the following:

$$q_{e(exp)} = q_{total}/x \quad (2)$$

W_{total} is calculated from Equation (3):

$$W_{total} = C_0 Q t_{total}/1000 \quad (3)$$

Y is the ratio of the maximum capacity of the column (q_{total}) to the total amount of vanadium sent to column (W_{total}).

$$Y = (q_{total}/W_{total}) \times 100 \quad (4)$$

Proper design of a column adsorption process needs prediction of the concentration-time profile or breakthrough curve for the outflow. Kinetic models were used to determine the dynamic process of the column.

2.5.1 Thomas model

The maximum adsorption capacity is needed in design. Usually, the Thomas model is used to accomplish the purpose. The info gathered from a column in continuous mode studies were used to determine the maximum solid phase quantity of vanadium on adsorbent and the adsorption rate constant needs the kinetic model made by Thomas (Thomas et al., 1944). The Thomas model is one complete general and widely used methods in column efficiency theory. The expression by Thomas for an adsorption column is given below:

$$\frac{C_t}{C_0} = \frac{1}{1+exp(\frac{k_{Th}q_e x}{Q-k_{Th}C_0 t})} \quad (5)$$

The adsorption capacity of the column q_e and the kinetic coefficient k_{Th} can be calculated from a plot of C_t/C_0 versus t for a given flow rate by doing a nonlinear regression analysis.

2.5.2 Adams–Bohart model

The Adams–Bohart model starts by assuming that the adsorption rate is related to both the residual capacity of the adsorbent and the concentration of the adsorbate. The Adams–Bohart model determines of the initial part of the breakthrough curve, shown as (Bohart et al.,1920):

$$\frac{C_t}{C_0} = \exp\left(k_{AB}C_0 t - k_{AB}N_0\frac{Z}{F}\right) \quad (6)$$

From this equation, values showing the behaviour of operational parameters of the column is given by a plot of C_t /C_0 versus t at a given bed depth and flow rate applying the nonlinear regressive method.

2.5.3 Yoon–Nelson model

The Yoon–Nelson is applied by assuming that the rate of lowering in the probability of adsorption for every adsorbate molecule is related to the adsorbate adsorption and the adsorbate breakthrough's probability on the adsorbent. The Yoon–Nelson model is less complicated compared to other models and also need no detailed info about the characteristics and the type of adsorbent, and the properties of the adsorption bed (Aksu et al., 2004). The Yoon–Nelson equation is given by (Yoon et al.,1984):

$$\frac{C_t}{C_0 - C_t} = \exp(k_{YN}t - \tau k_{YN}) \quad (7)$$

The approach involves a plot of C_t /(C_0–C_t) against time (t) given in Equation (7). k_{YN} and τ is given by applying a nonlinear regressive method.

2.5.4 Clark model

The Clark is a new simulation of breakthrough curves (Clark et al., 1987). The model made by Clark was about the use of a mass-transfer concept in combined with the Freundlich isotherm (Clark et al., 1987):

$$\frac{C_t}{C_0} = (\frac{1}{1+Ae^{-rt}})^{1/(n-1)} \quad (8)$$

By a plot of C_t /C_0 versus *t* at a given bed depth and flow rate applying nonlinear regressive analysis to find *A* and *r* values.

2.5.5 Bed-depth or service time analysis (BDST) model

BDST is an uncomplicated model for predicting the correlation between bed height Z, and service time t, with processing concentrations and adsorption parameters. The BDST model is about assuming that the amount of adsorption is controllable by the reaction surface between adsorbate and the capacity unused of the adsorbent (Goel et al., 2005).

The breakthrough time determined for various bed depths used in this study were given into the BDST model. A linear correlation between bed height and service time is in equatıon (9) (Goel et al., 2005):

$$t = \frac{N_0'}{C_0 F} Z - \frac{1}{K_a C_0} \ln(\frac{C_0}{C_t} - 1) \quad (9)$$

From the plot of t versus. Z should give a straight line with No the adsorption capacity and Ko the rate constant can be calculated.

A simple form of the BDST model is

$$t=aZ-b \quad (10)$$

In which

$$a = \frac{N_0'}{C_0 F} \quad (11)$$

$$b = \frac{1}{K_a C_0} ln(\frac{C_0}{C_t} - 1) \quad (12)$$

The slope constant for another flow rate is calculated by equatıon. (13):

$$a' = \frac{aF}{F'} = aQ/Q' \quad (13)$$

where a value and F value are the previous slope and influent linear velocity and a' value and F' value are the present slope and influent linear velocity, respectively. When the column used in the experiment is the same column in dimensions, the original (F) and the new influent linear velocity's (F') ratio and original flow rate (Q) and the new flow rate's (Q') ratio are the same. For any other concentrations, the wanted equation is determined by a new slope and intercept with the following equations:

$$a' = aC_0/C_0' \quad (14)$$

$$b' = b * \frac{C_0}{C_0'} * \frac{\ln(\frac{C_0'}{C_f^{-1}})}{\ln(\frac{C_0}{C_{f^{-1}}})} \quad (15)$$

b', b are the present and previous intercepts, respectively and C_0' and C_0 are the present and previous concentrations, respectively. C_f is the outflow concentration at inflow concentration C_0' and C_f is the outflow concentration at inflow concentration C_0.

3 MATERIALS AND METHODS

3.1 CHEMICALS

Glycidyl methacrylate (GMA), ethylene glycol dimetahacrylate (EGDM), benzoyl peroxide (BPO), mercury (II) nitrate -Hg $(NO_3)_2$, gallic acid $H_6C_7O_5$, ammonium metavanadate NH_4VO_3 any other chemicals were "pure" and or "analytical" grade and purchased from Merck. The pH was adjusted with dilute HCl or NaOH solutions and in all experiments distilled water was used. Bulk polymerization method was used for accumulating of detached radical crosslinking polymerization of GMA having EGDM with a gram molecule ratio 9:1. The provoker, reaction degree of heat, and time were elected as BPO (1% mole), 80^oC and 3h, respectively. After doing a purification procedure giving disintegration in front of cold methanol as non-solvent, and cleaning with ethanol or methanol mixture, the collected poly(glycidyl methacrylate (pGMA) powders dried-out at 30^oC under reduced pressure. In the second part of the process, the amination process of pGMA was done by epoxy ring opening process. To get amino functionalized pGMA resin, 1 g pGMA, and 10 ml dimethylformamide (DMF) were put into a 25 ml test tube and the reaction solution degassed for 15 minutes with nitrogen. Thus, 4 g of EDA was put into the reaction mixture and the closed air-tight test tube submerged in a stable bath at 80^oC.12 hours later, this mixture product was filtered and washed independently with ethanol three times, ethanol or water (50:50, w:w) solution, and water, respectively. The product was dried-out at 25^oC in an oven, milled then sieved. The sieved parts that had a particle size of 350-500 mesh was taken for using in adsorption experiments.

3.2 GENERAL ADSORPTION STUDIES AND PROCEDURE

Continuous flow adsorption experiments were done in a glass column (2 cm internal diameter and 50 cm height). A series of experiments was done with ammonium metavanadate NH_4VO_3 and amino functionalized polymers columns. Amino functionalized polymers were put in the glass column. First, the adsorbent in the column was 2g (3 cm). The vanadium solution of

100mg/L has been pumped to the column in a up-flow direction using a peristaltic pump at 7.5, 10 then 12.5 ml/min, respectively. Samples were collected at regular intervals of 10 minutes in all the adsorption. The concentration of vanadium in the effluent was analysed with a spectrophotometer by monitoring the absorbance changes at a wavelength of maximum absorbance (415 nm). The calibration curves were the plot between absorbance and concentration of the vanadium. After each 10 minutes a collection was made then the standard of made for that specific collection by diluting it at 1ml to 100ml of water twice to give 0.010µgV. Once the standard solution was made 1ml of Hg $(NO_3)_2$ was immediately add to the standard then put in a water bath regulated to 25°C ± 0.5°C for 30 to 45 minutes. After that, the sample was removed from the bath then 1ml of NaH_2SO_4 was added to it then swirled to mix thoroughly for 1 min then 1ml of Gallic acid was added then the sample was return to the bath for 60 minutes. At the end of those 60 minutes sample was collected its absorbance was measured with the spectrophotometer. The pH was kept at 4.5 throughout the experiment. The calibration curve is shown in Figure 2.

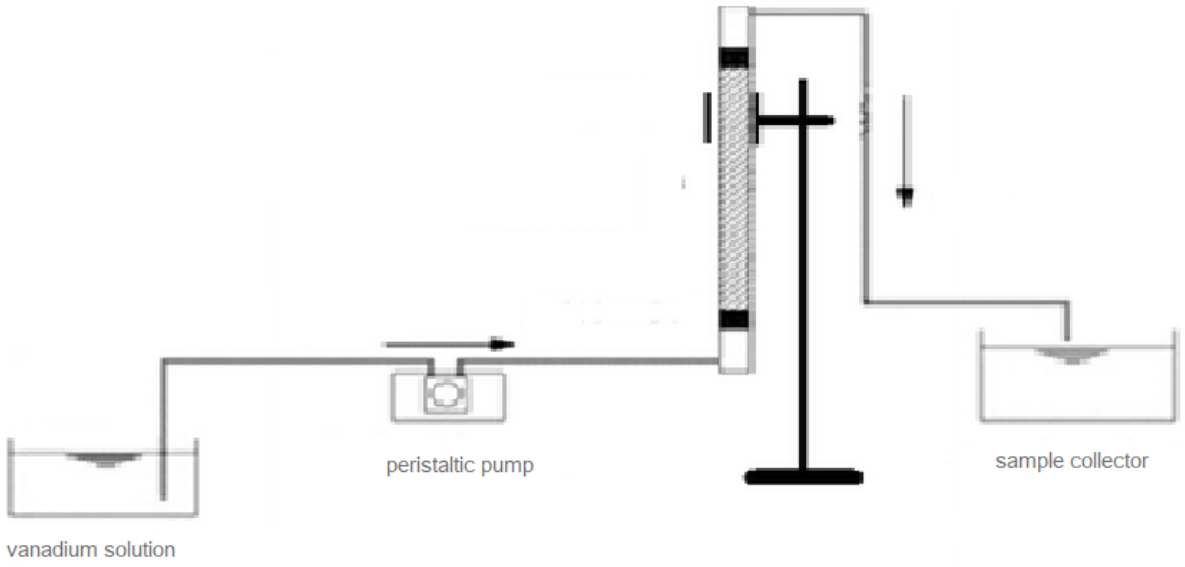


Figure 1. Fixed bed column

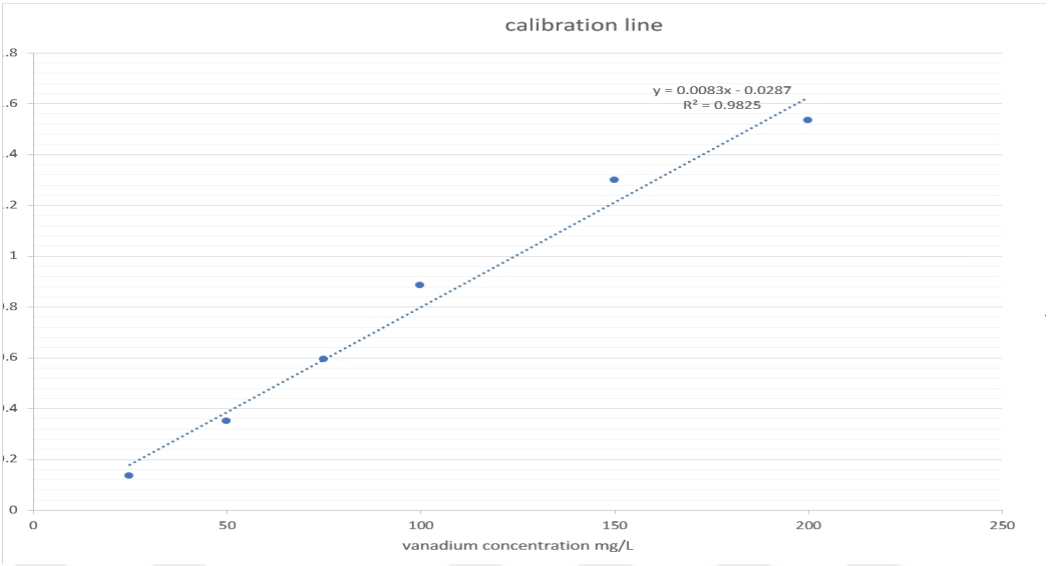


Figure 2**:** Calibration line of vanadium concentration

The removal efficiency was examined with Equation 16.

$$q_e = \frac{(C_o - C_e)}{m} \times V \qquad (16)$$

Where C_o is concentration at t = 0 of ions (mg/L), C_e is the concentration at equilibrium (mg/L), q_e amount adsorption equilibrium (mg/g), as m is the adsorbent's mass (g), and V is the volume.

4 RESULTS AND DISCUSSION

4.1 EFFECTS ON THE BREAKTHROUGH CURVE

4.1.1 Effect of the flow rate on the breakthrough curve

After the first group of experiments as shown in the Figure 3 which were at different the flow rates. We see that when the flow rate gets higher the breakthrough occurs considerably faster than when the flow rate is slower then we observed a much better adsorption. The Vanadium when exposed to a faster flow rate was not able to sustain long removal which was the result of an early breakthrough occurrence but when the flow rate was slowed the Vanadium was able to sustain a longer and greater removal which was the result of a slower flow.

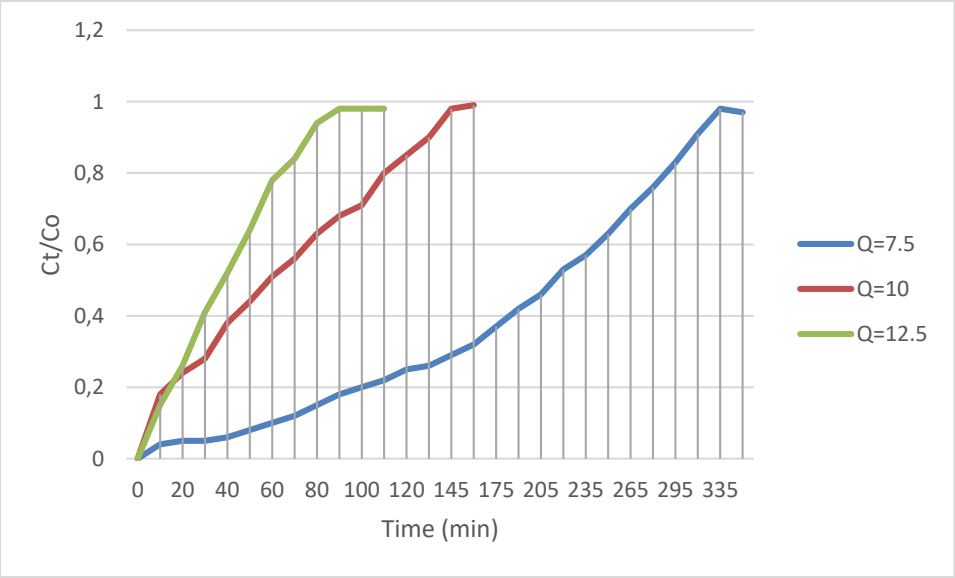


Figure 3: Breakthrough curves plot: the effect of flow rate on the vanadium adsorption.

(Co=75 mg/l, Z=3cm).

4.1.2 Effect of the concentration on the breakthrough curve

The effect of inflow Vanadium concentration on the shape of the breakthrough curves is shown in Figure 4. It is shown that the breakthrough time lowers with increasing influent Vanadium

amount. At lower inflow of Vanadium concentrations, breakthrough curves were spread and breakthrough happen slower. As inflow concentration increased, defined breakthrough curves were observed. These results illustrate that the change of concentration values affects the saturation speed and breakthrough occurrence. This is due the fact that more adsorption sites were being saturated as the Vanadium concentration elevates.

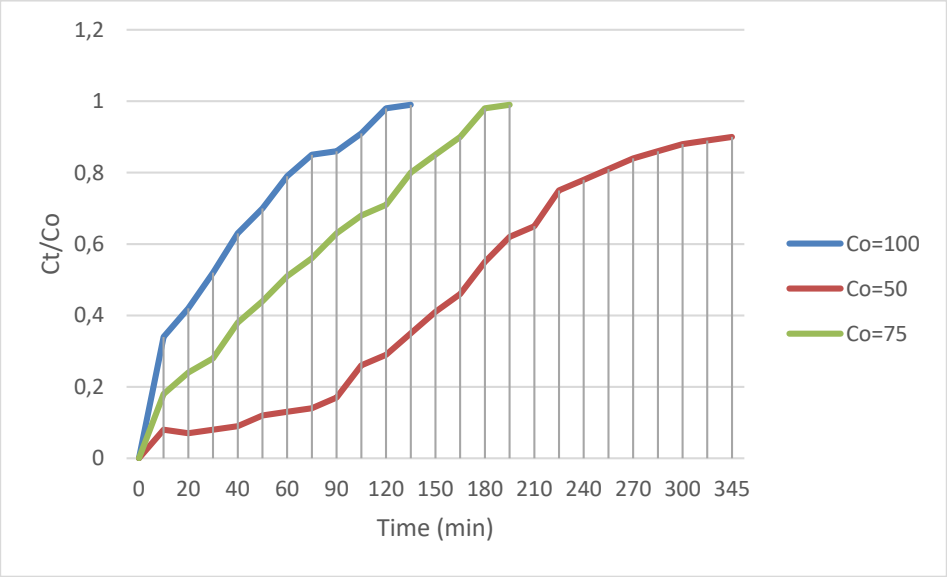


Figure 4: Breakthrough curve: the effect of influent concentration on Vanadium adsorption (Q = 10 ml/min, Z=3cm).

4.1.3 Effect of different bed depth on the breakthrough curve

The breakthrough curves at different bed heights are shown in Figure 5 where it is shown that as the bed depth (adsorbent mass) becomes higher, Vanadium had more time in contact with aminated beads that gives it a higher removal in the column of Vanadium molecules. So the more bed depth increased column resulted in a lower in the outflow concentration at the same

service time. The a of the breakthrough curve lowers with higher bed height, which gives broadened mass transfer zone. High uptake was seen at the longest bed depth. Result of a larger surface area of adsorbent, which give a bigger number of binding sites for adsorption (Z.Zulfadhly, M.D Mashitah et al. 2001). The adsorption info were calculated and the Vanadium taken and extraction percent's considering the flow rate, inflow Vanadium concentration and bed heights are presented in Table 1. From Table 1, the value of Y lowered with higher flow rates. Even though the value of qe became higher with increasing inflow concentration, the value of Y seen had an opposite trend. But with higher bed depth, both qe and Y augmented.

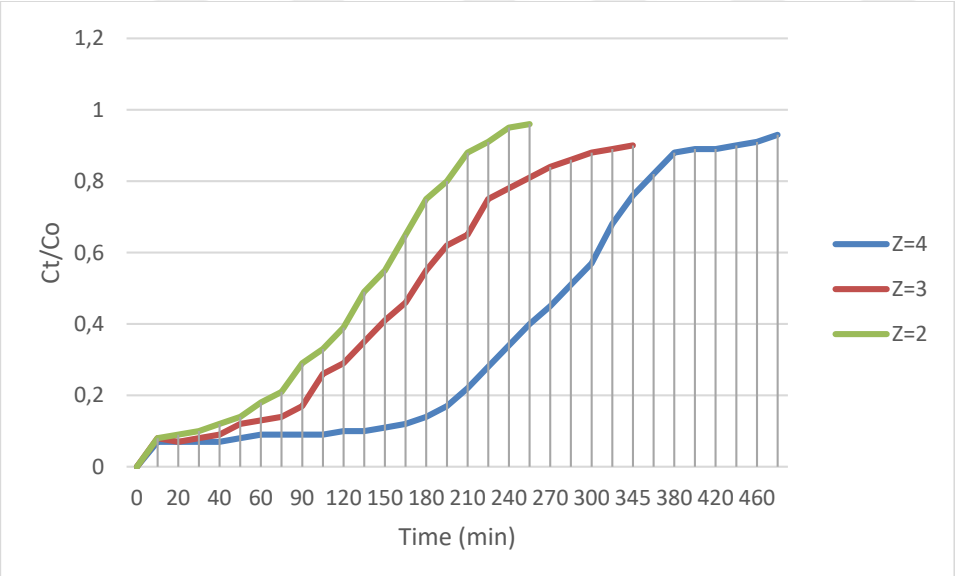


Figure 5. Breakthrough curves: the effect of different bed depths on Vanadium adsorption (Co = 50 mg/ml, Q = 10 ml/min).

4.2 DISCUSSION

A proper design of a column adsorption process needs to have prediction of the concentration to time profile or the breakthrough curve for the outflow. To describe the fixed-bed column behavior and to scale up it for industrial applications, Yoon–Nelson and Thomas were utilised to get the kinetic model inside column and to approximate breakthrough curves. The BDST model can predict the breakthrough curves for other experiments too at different conditions.

4.2.1 Thomas model

The column data were applied to the Thomas model to get the Thomas rate constant (k_{Th}) and solid-phase concentration (q_e). The obtained coefficients (R^2), correlation constants were found by applying nonlinear regression. The results are given in Table 1 where values of R^2 go from 0.93 to 0.99. So the correlation between C_t/C_0 and t in to Equation (5) is high. Table 1 shows that as the inflow concentration increased, the value of q_e get bigger but k_{Th} becomes smaller. This is due to the driving force for adsorption is the concentration difference between the vanadium on the adsorbent and the vanadium in the solution (Z. Aksu and F. Gonen et al. 2004, R.P. Han, J.H. Zhang et al. 2006). Hence the big driving force is a result of the higher Vanadium amount giving a better column performance. With flow rate becoming higher, the value of q_e lowered but the value of k_{Th} became higher. While the bed height increased, the value of q_e became significantly larger as the value of k_{Th} lowered significantly. Thus lower flow rate and increased inflow concentration would make better adsorption of Vanadium on the amino functionalized polymer column. Comparing q_e theoretical and experimental showed that they were close considering experimental conditions. The predicted curves at different experimental

conditions conforming to the Thomas model are given in Figs. 6 to 23. The figures showed that there was a good similarity between the experimental and theoretical points predicted. The

Thomas model is valid for adsorption reactions in which the external and internal diffusions are not the limiting step (Z. Aksu and F. Gonen et al. 2004)

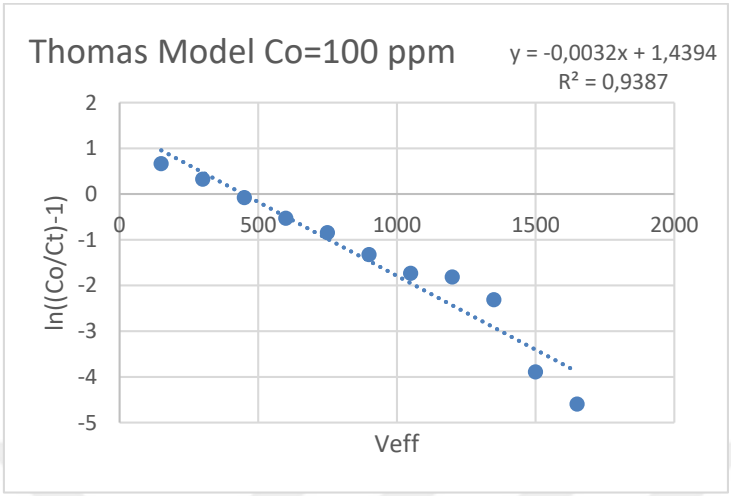


Figure 6: Thomas model graph K_{Th} and q_o values

K_{Th} = 0.32 (ml min^{-1} g^{-1})

q_o = 22.50 (mg g^{-1})

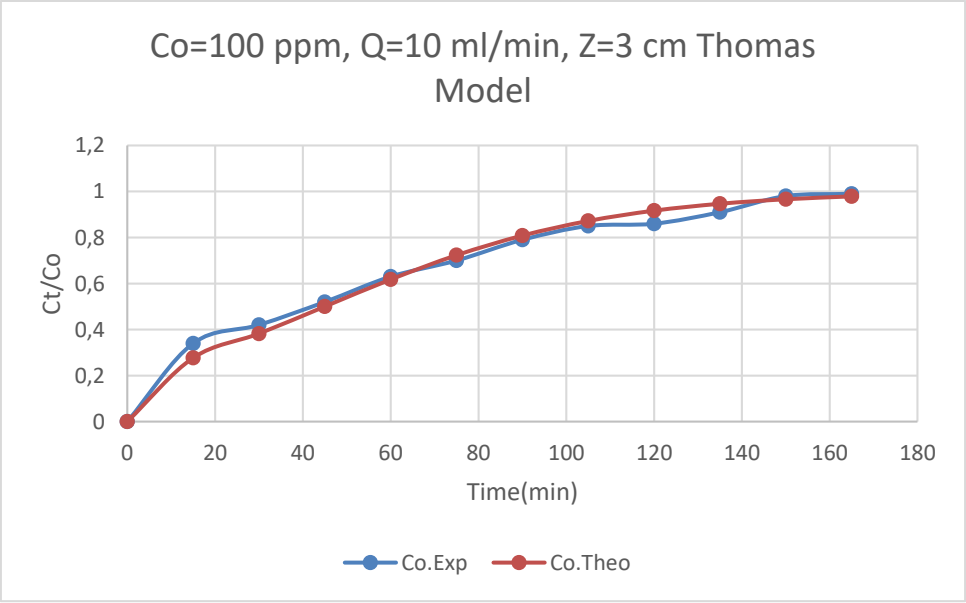


Figure 7: Comparison of experimental value to theoretical value at

Co=100 ppm, Q=10 ml/min, Z=3 cm Thomas Model

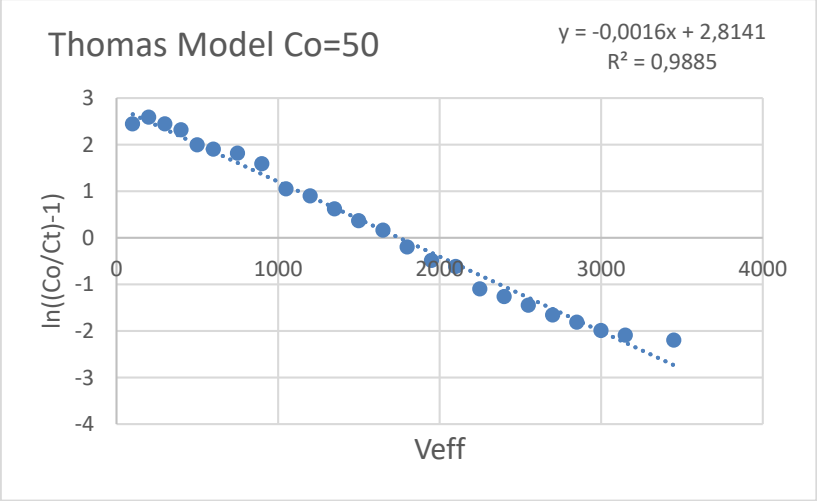


Figure 8: Thomas model graph K_{Th} and q_o values

K_{Th} = 0.32 (ml min^{-1} g^{-1})

q_o = 43.97 (mg g^{-1})

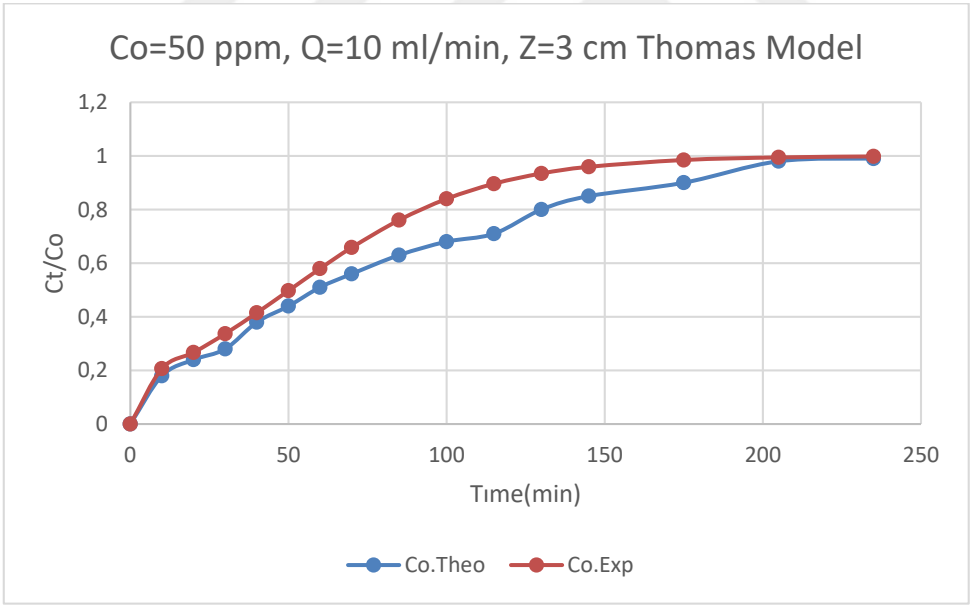


Figure 9: Comparison of experimental value to theoretical value at

Co=50 ppm, Q=10 ml/min, Z=3 cm Thomas Model

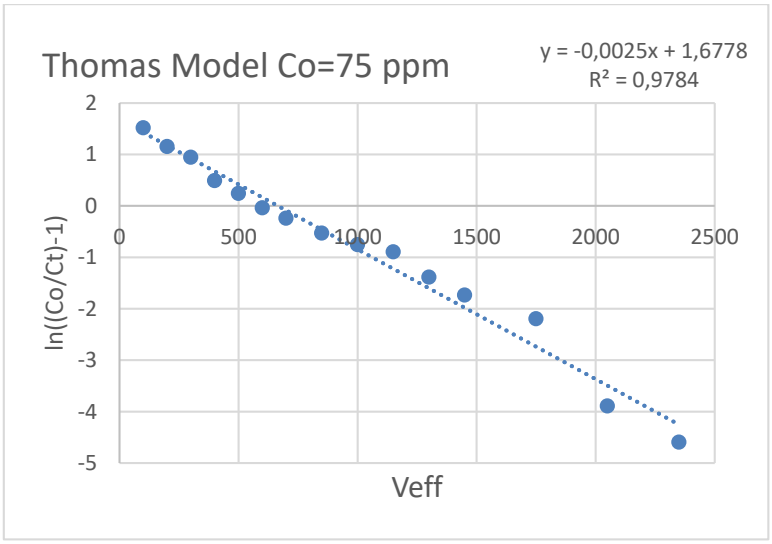


Figure 10: Thomas model graph K_{Th} and q_o values

K_{Th} = 0.33 (ml min^{-1} g^{-1})

q_o = 25.167 (mg g^{-1})

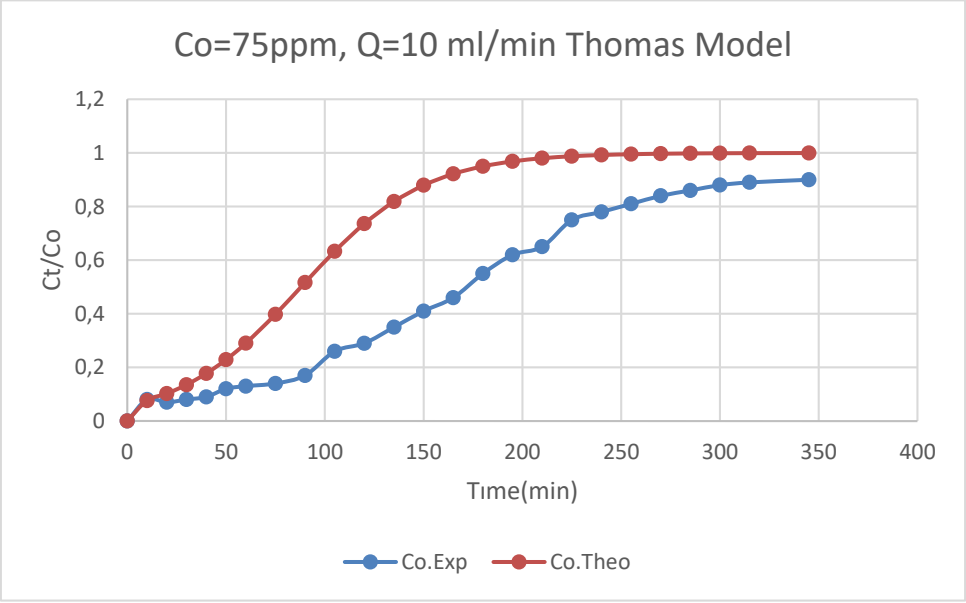


Figure 11: Comparison of experimental value to theoretical value at

Co=75 ppm, Q=10 ml/min, Z=3 cm Thomas Model

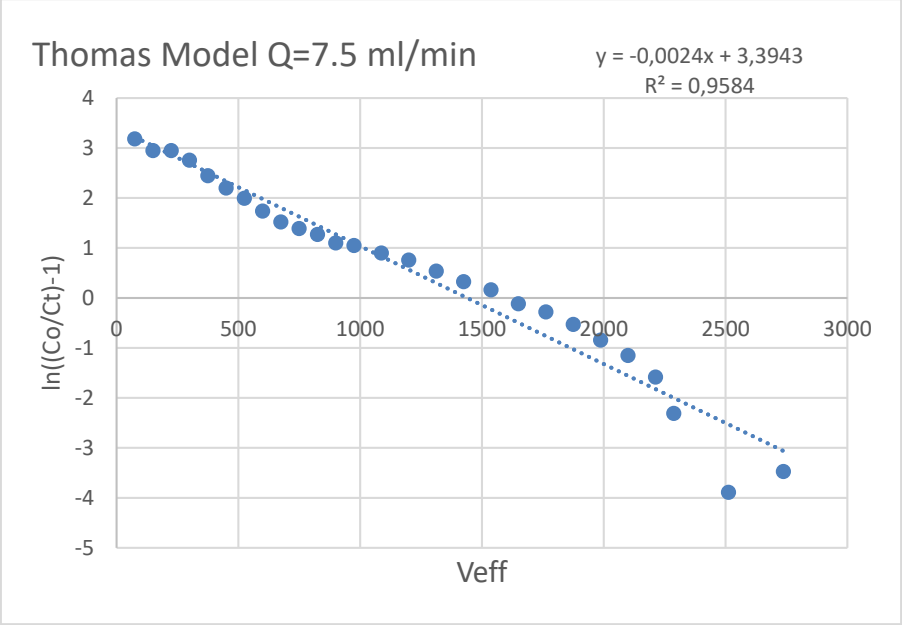


Figure 12: Thomas model graph K_{Th} and q_o values

K_{Th} = 0.24 (ml min^{-1} g^{-1})

q_o = 53.04 (mg g^{-1})

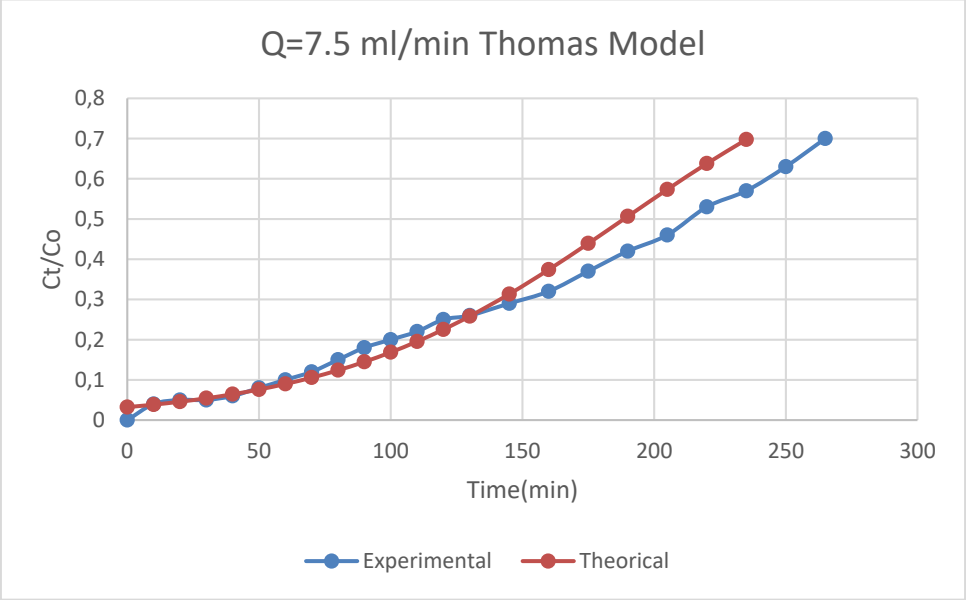


Figure 13: Comparison of experimental value to theoretical value at

Co=75 ppm, Q=7.5 ml/min, Z=3 cm Thomas Model

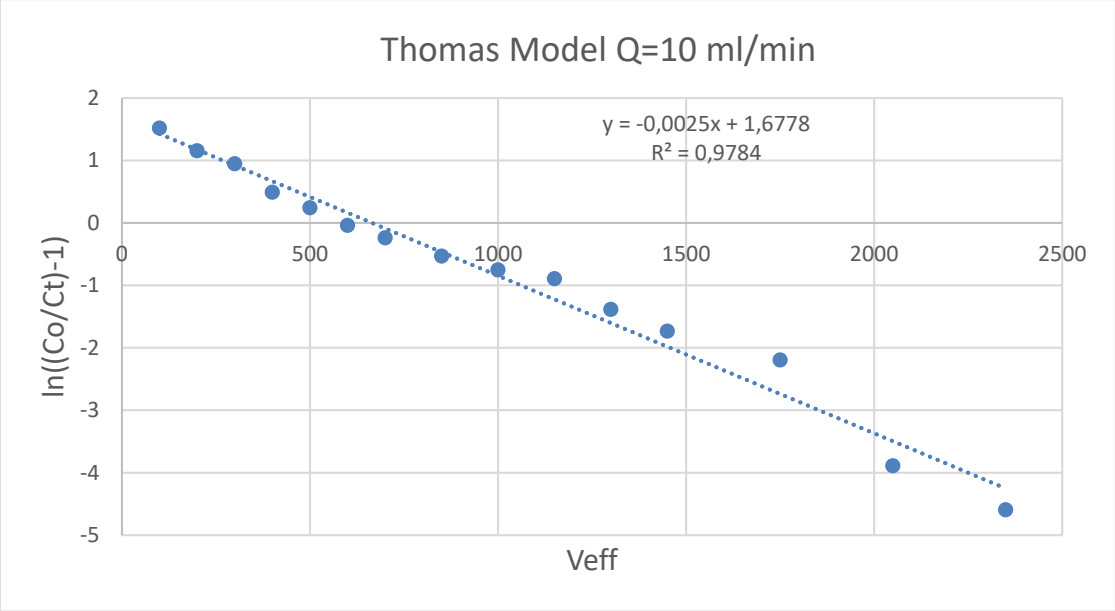


Figure 14: Thomas model graph K_{Th} and q_o values

K_{Th} = 0.33 (ml min^{-1} g^{-1})

q_o = 25.167 (mg g^{-1})

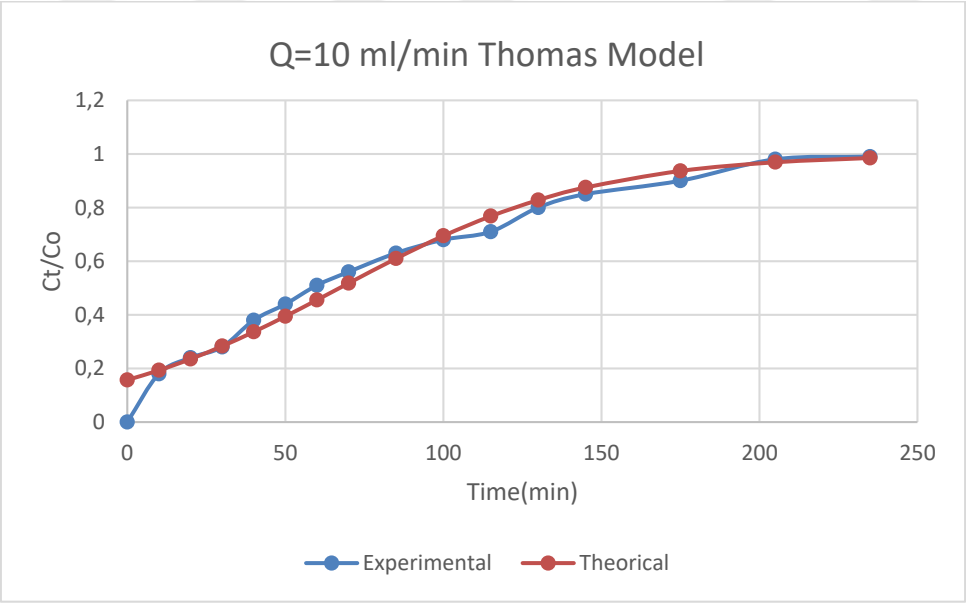


Figure 15: Comparison of experimental value to theoretical value at

Co=75 ppm, Q=10 ml/min, Z=3 cm Thomas Model

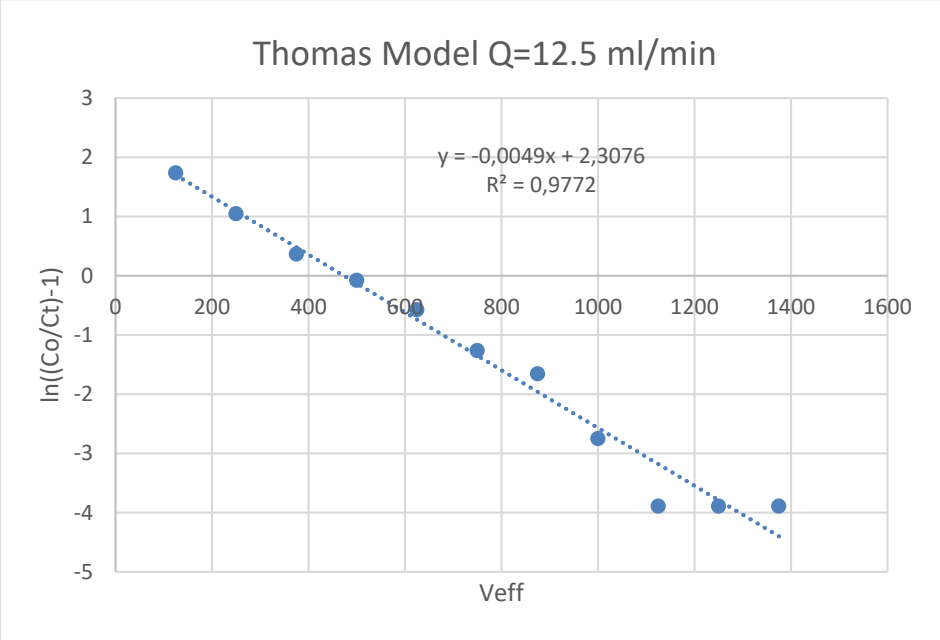


Figure 16: Thomas model graph K_{Th} and q_o values

K_{Th} = 0.81 (ml min^{-1} g^{-1})

q_o = 17.66 (mg g^{-1})

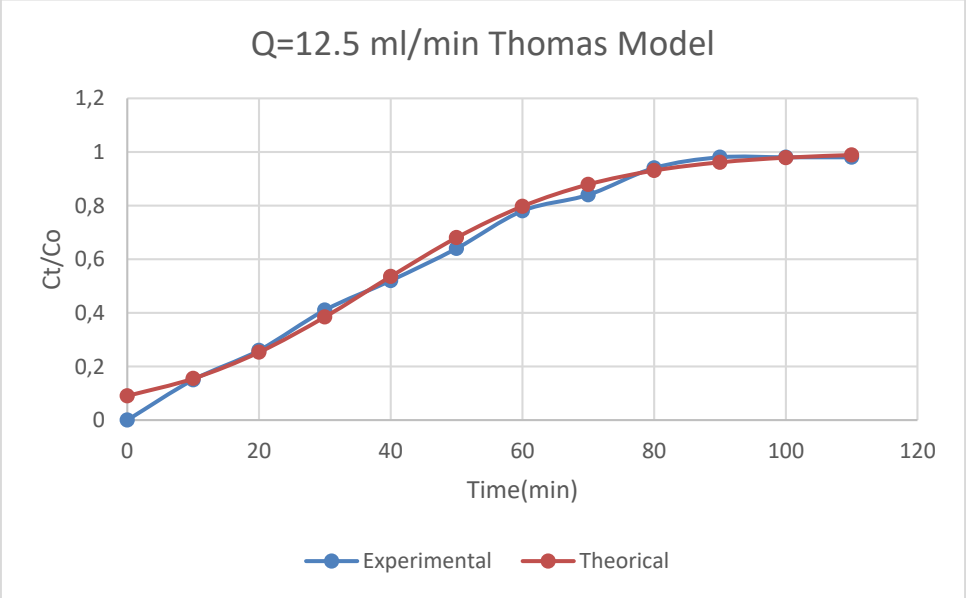


Figure 17: Comparison of experimental value to theoretical value at

Co=75 ppm, Q=12.5 ml/min, Z=3 cm Thomas Model

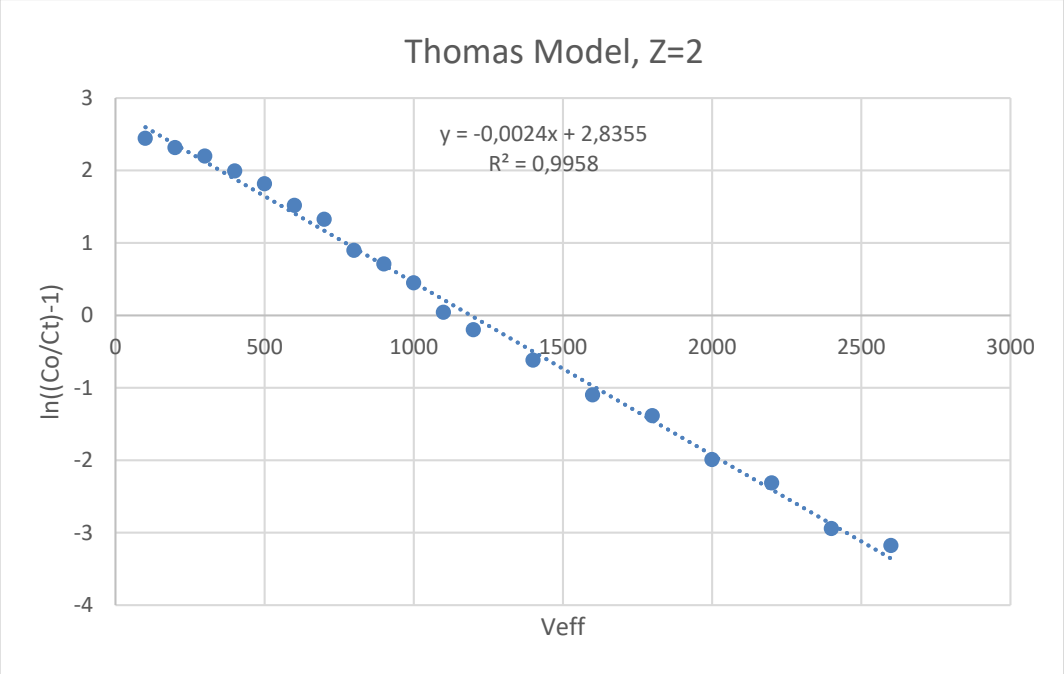


Figure 18: Thomas model graph K_{Th} and q_o values

K_{Th} = 0.32 (ml min^{-1} g^{-1})

q_o = 43.97 (mg g^{-1})

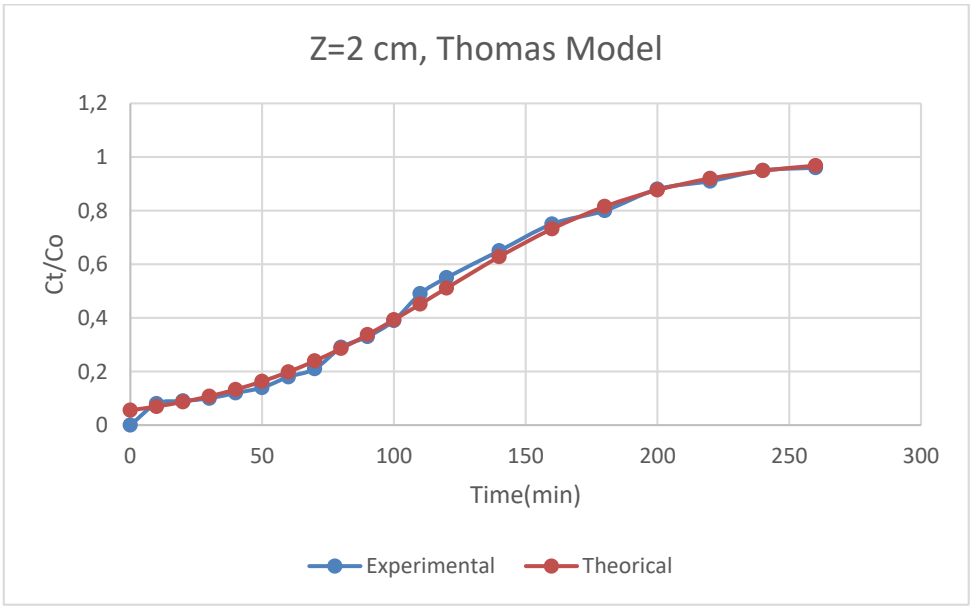


Figure 19: Comparison of experimental value to theoretical value at

Co=50 ppm, Q=10 ml/min, Z=2 cm Thomas Model

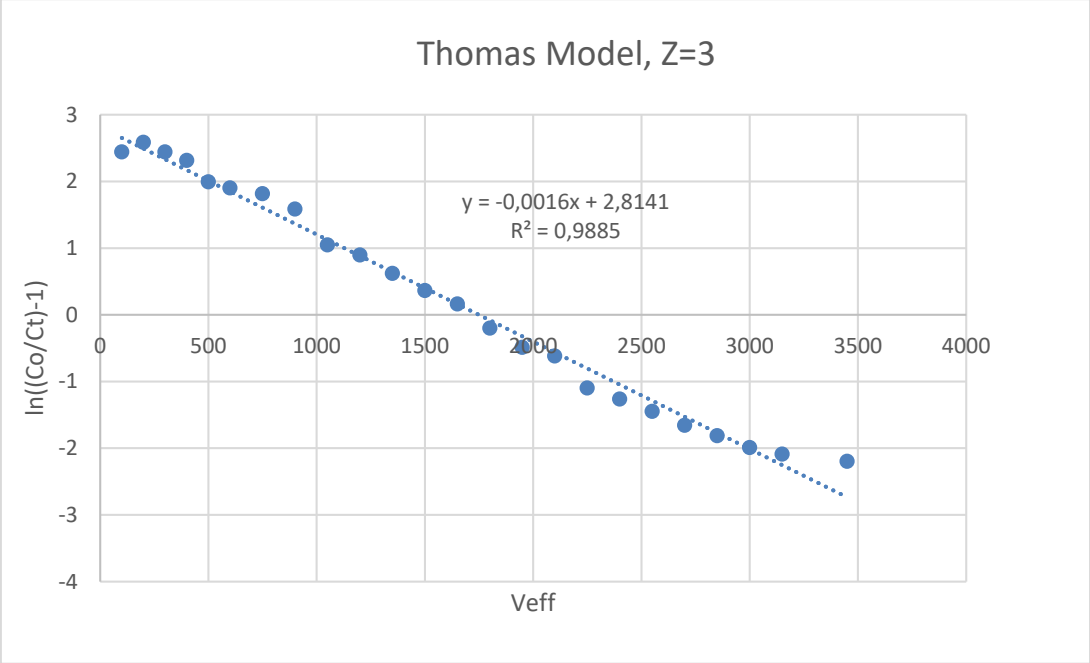


Figure 20: Thomas model graph K_{Th} and q_o values

K_{Th} = 0.48 (ml min^{-1} g^{-1})

q_o = 44.30 (mg g^{-1})

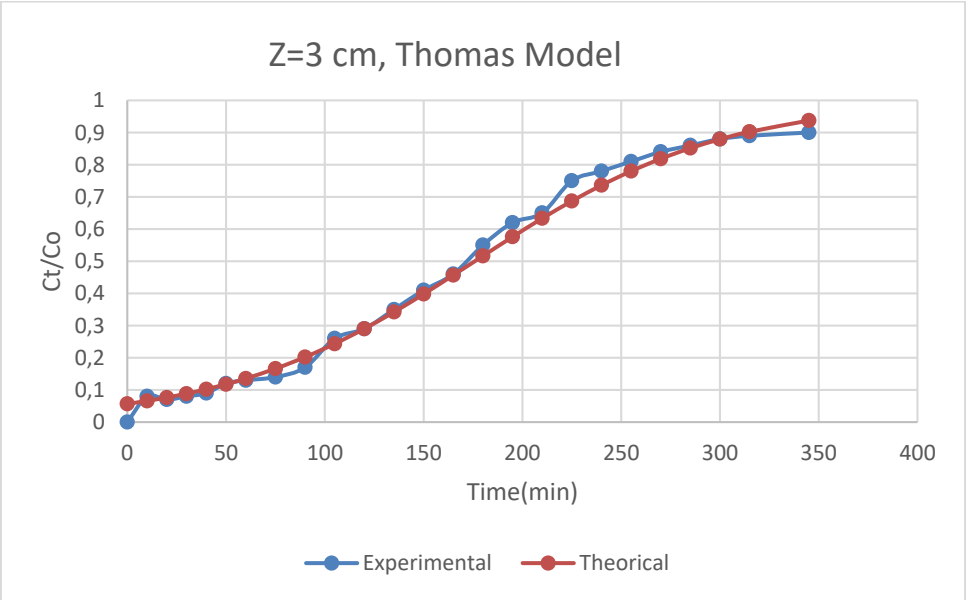


Figure 21: Comparison of experimental value to theoretical value at

Co=50 ppm, Q=10 ml/min, Z=3 cm Thomas Model

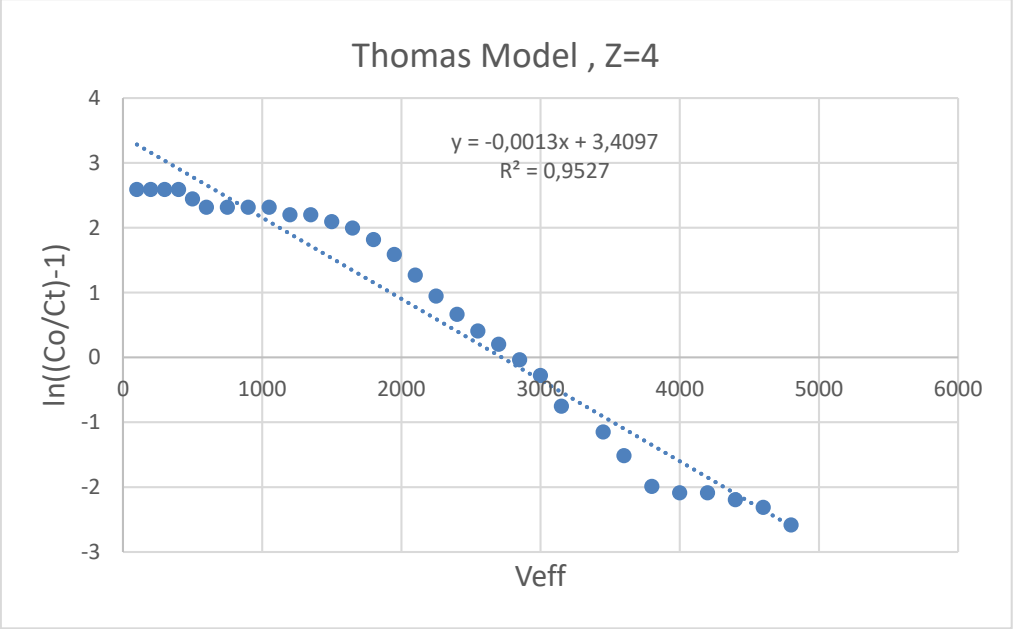


Figure 22: Thomas model graph K_{Th} and q_o values

K_{Th} = 0.26 (ml min^{-1} g^{-1})

q_o = 49.17 (mg g^{-1})

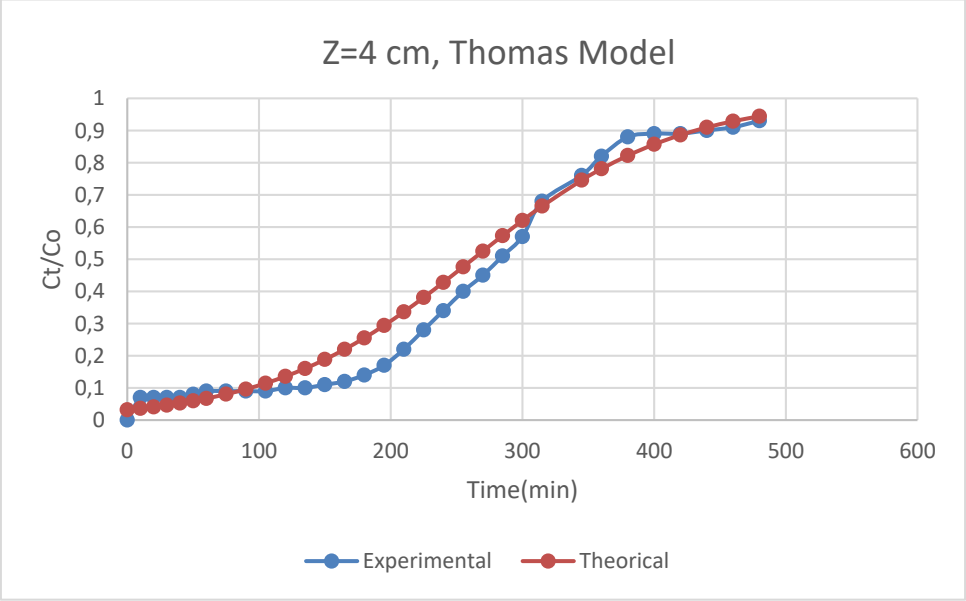


Figure 23: Comparison of experimental value to theoretical value at

Co=50 ppm, Q=10 ml/min, Z=4 cm Thomas Model

Table 1 : Parameters of Thomas model applying nonlinear regression analysis and the equilibrium Vanadium uptake (q_e) and the Thomas rate constant (k_{Th}) for Vanadium adsorption to aminated beads under different conditions

C_0, (mg/l)	Q, (ml/min)	Z, (cm)	$k_{Th}(x10^2)$, (ml $min^{-1}mg^{-1}$)	q_e, (mg g^{-1})	R^2,
50	10	3	32	43.97	0.98
75	10	3	33	25.16	0.97
100	10	3	32	22.50	0.93
75	7.5	3	24	53.03	0.95
75	12	3	81.67	17.66	0.97
50	10	2	42	43.04	0.93
50	10	4	22	46.67	0.99

4.2.2 Yoon–Nelson model

An elementary theoretical model made by Yoon–Nelson was applied to observe the breakthrough behavior of Vanadium on the amino functionalized polymer. So the values of k_{YN} and τ, the rate constant and the time required for 50% Vanadium breakthrough, respectively, could be calculated. The values of k_{YN} and τ are given in Table 2. As shown in the table, as k_{YN} the rate constant increased and τ the 50% breakthrough time decreased with both higher flow rates and higher concentrations. When the bed depth got longer, the values of τ did too while the values of k_{YN} lowered. The info in Table 2 also shows that values of τ are alike compared to the experimental results, only the initial concentrations of 75 mg l^{-1} and

100 mg l^{-1} at Q = 10 ml min^{-1} and Z = 3 cm is different. The comparison between experimental and theoretical points according to the Yoon– Nelson model are seen in Figures. 24 to 41 at different conditions. The breakthrough curves of the experimental points were not

close to those predicted by the Yoon–Nelson model. So the correlation between the experimental and predicted values using the Yoon–Nelson model deviated significantly.

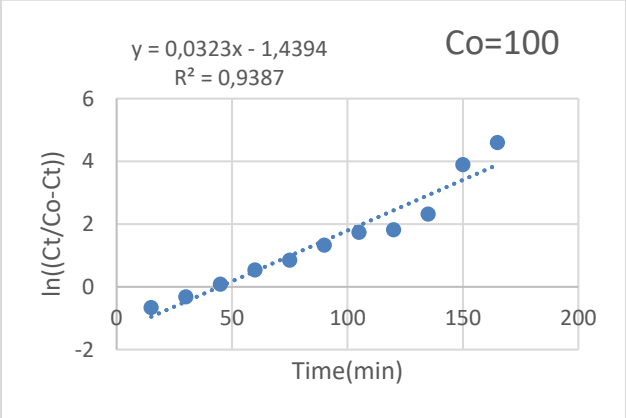


Figure 24: Yoon–Nelson model graph K_{YN} and τ values

K_{YN} = 0.032 (ml min^{-1} g^{-1})

τ = 44.51 (mg g^{-1})

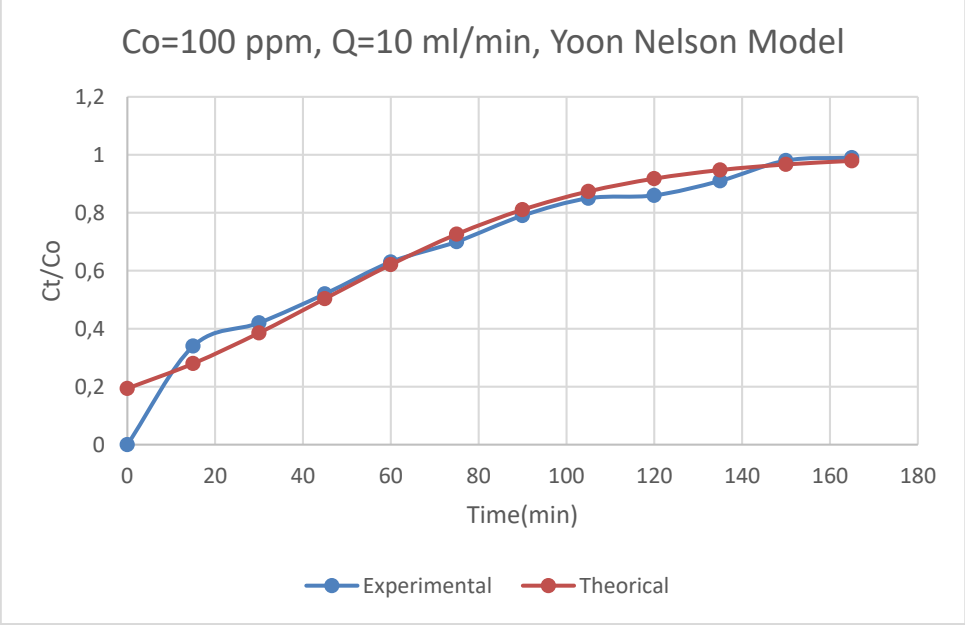


Figure 25: Comparison of experimental value to theoritical value at Co=100 ppm, Q=10 ml/min, Z=3 cm Yoon–Nelson model.

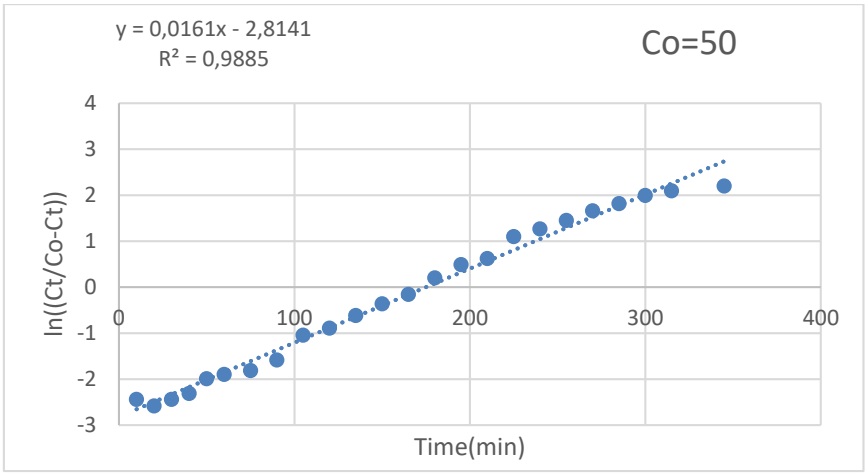


Figure 26: Yoon–Nelson model graph K_{YN} and τ values

K_{YN} = 0.016 (ml min^{-1} g^{-1})

τ = 175.88 (mg g^{-1})

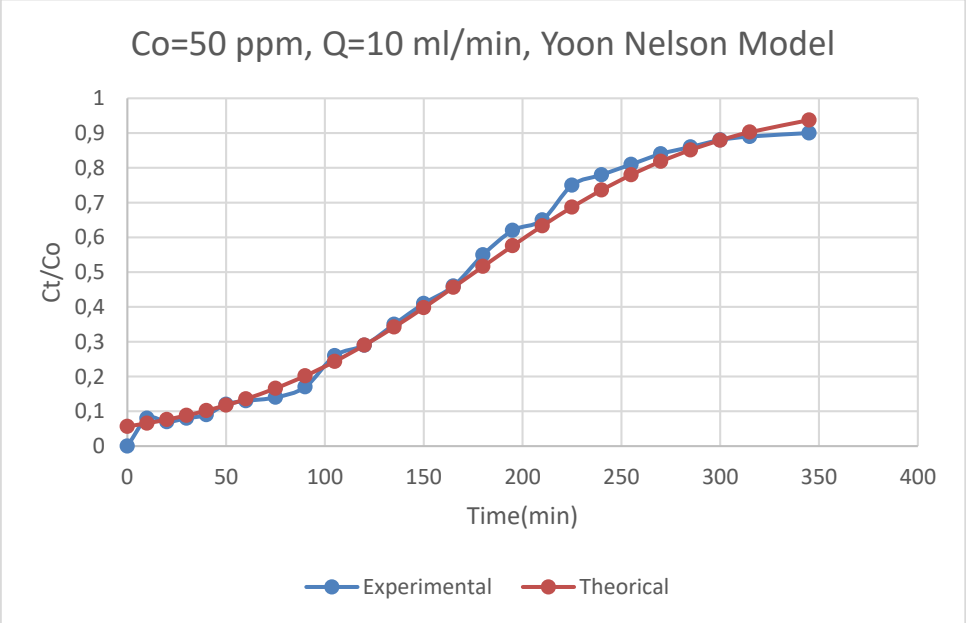


Figure 27: Comparison of experimental value to theoritical value at

Co=50 ppm, Q=10 ml/min, Z=3 cm Yoon–Nelson model

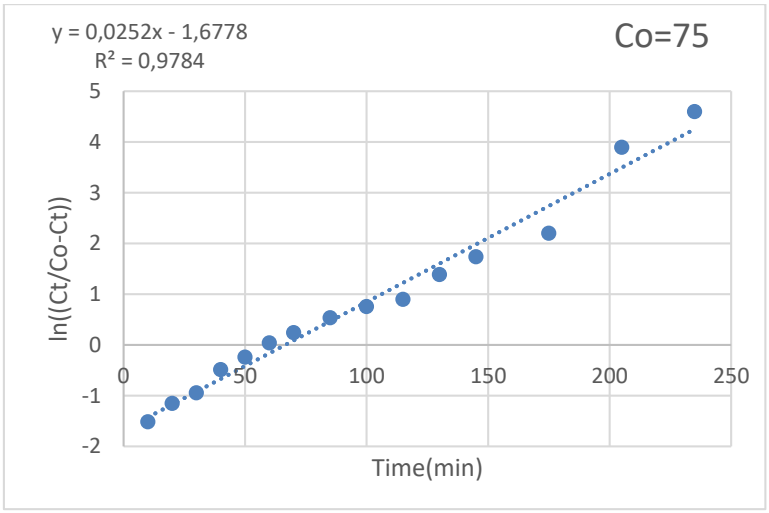


Figure 28: Yoon–Nelson model graph K_{YN} and τ values

K_{YN} = 0.025 (ml min^{-1} g^{-1})

τ = 67.2 (mg g^{-1})

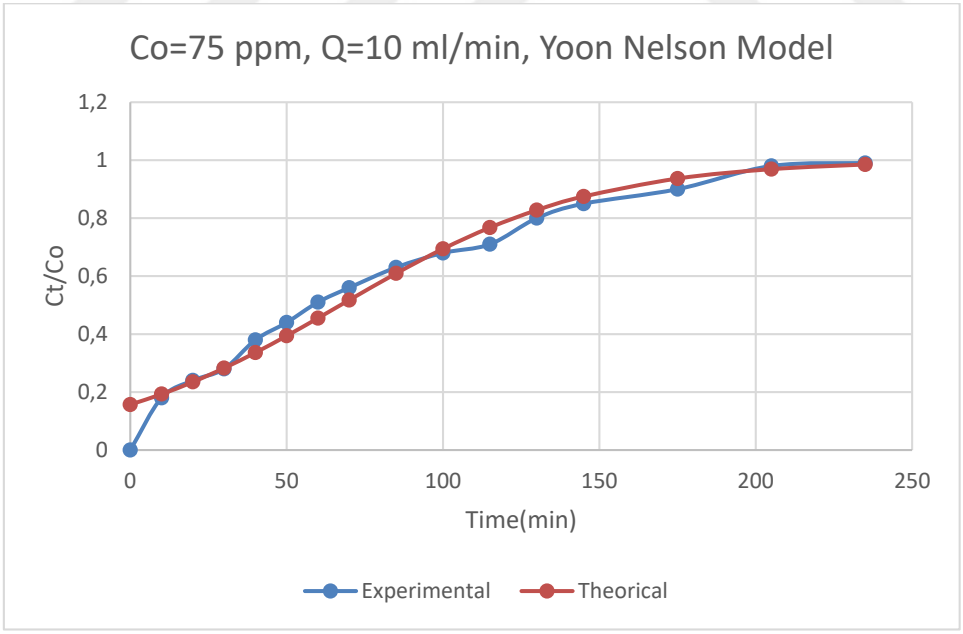


Figure 29: Comparison of experimental value to theoritical value at

Co=75 ppm, Q=10 ml/min, Z=3 cm Yoon–Nelson model

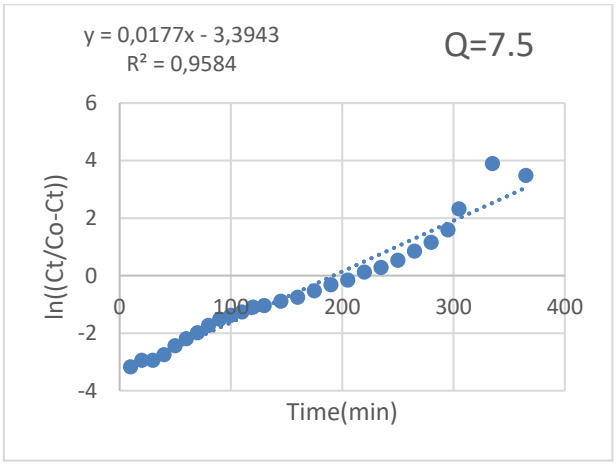


Figure 30: Yoon–Nelson model graph K_{YN} and τ values

K_{YN} = 0.017 (ml min^{-1} g^{-1})

τ = 199.64 (mg g^{-1})

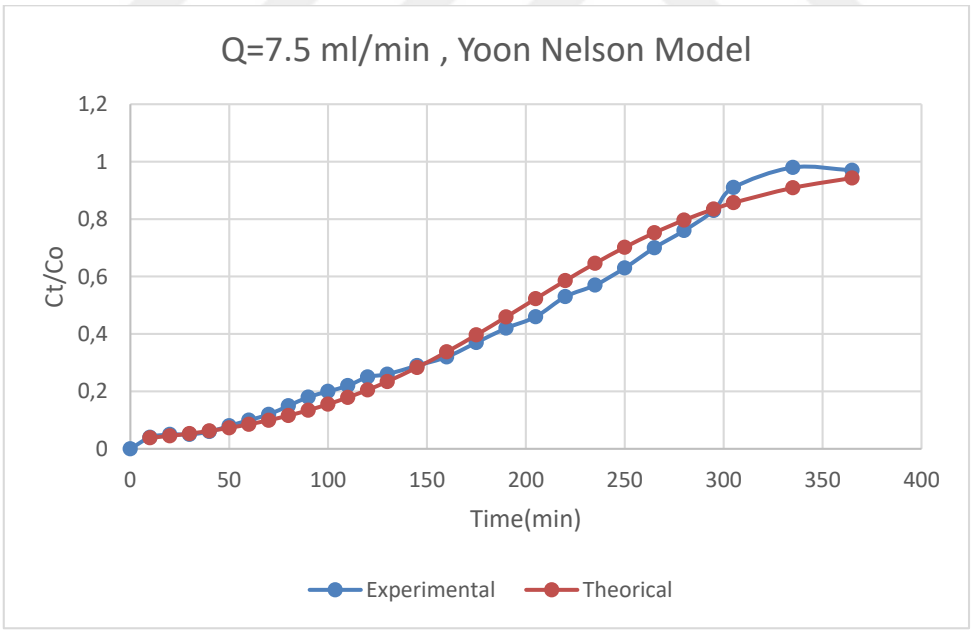


Figure 31: Comparison of experimental value to theoritical value at

Co=75 ppm, Q=7.5 ml/min, Z=3 cm Yoon–Nelson model

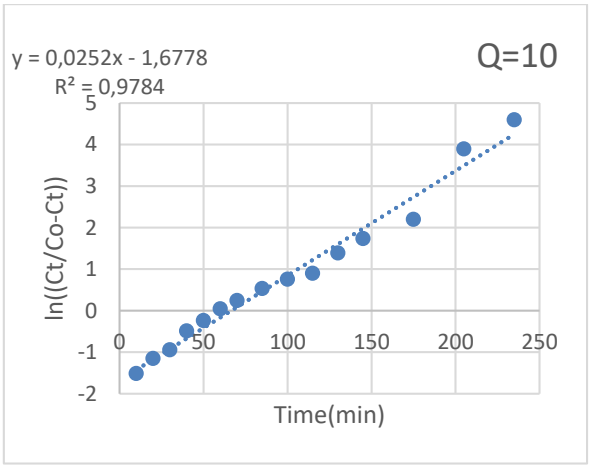


Figure 32: Yoon–Nelson model graph K_{YN} and τ values

$K_{YN} = 0.025$ (ml min^{-1} g^{-1})

$\tau = 67.2$ (mg g^{-1})

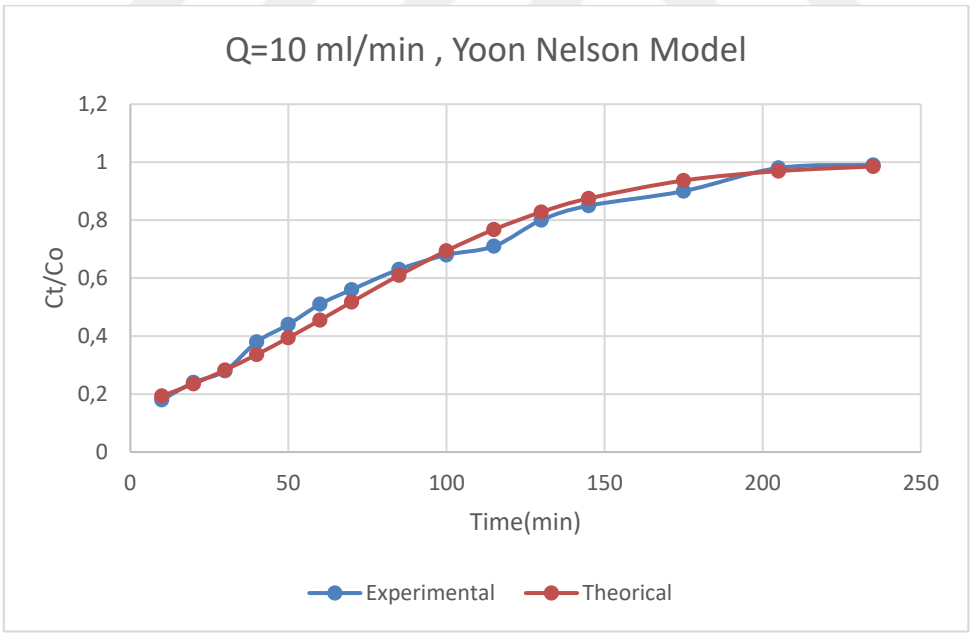


Figure 33: Comparison of experimental value to theoritical value at

Co=75 ppm, Q=10 ml/min, Z=3 cm Yoon–Nelson model

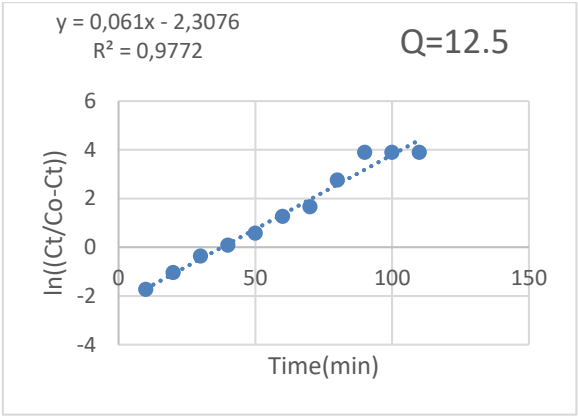


Figure 34: Yoon–Nelson model graph K_{YN} and τ values

$K_{YN} = 0.061$ (ml min^{-1} g^{-1})

$\tau = 37.81$ (mg g^{-1})

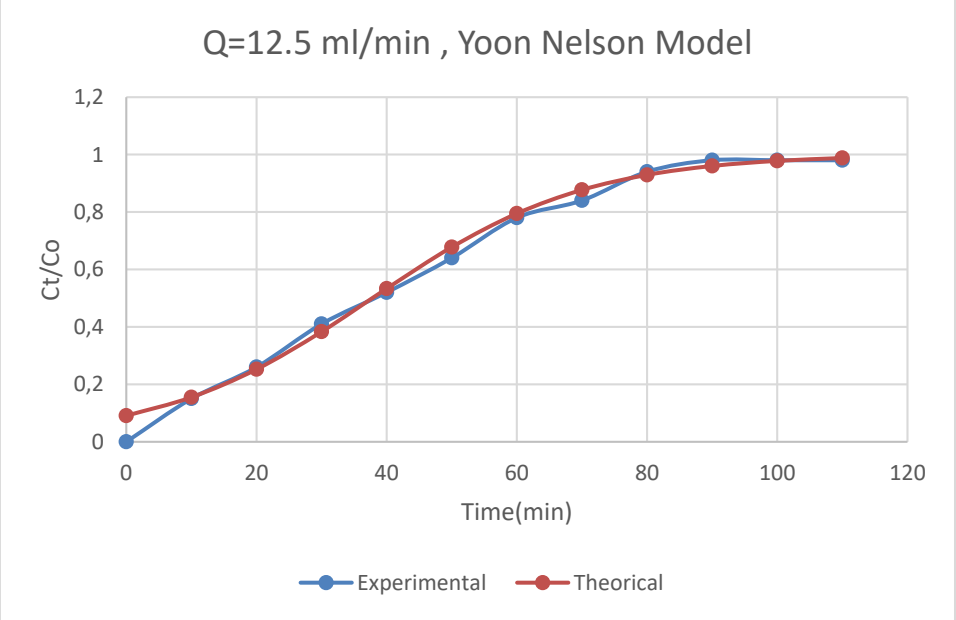


Figure 35: Comparison of experimental value to Theoritical value at

Co=75 ppm, Q=12.5 ml/min, Z=3 cm Yoon–Nelson model.

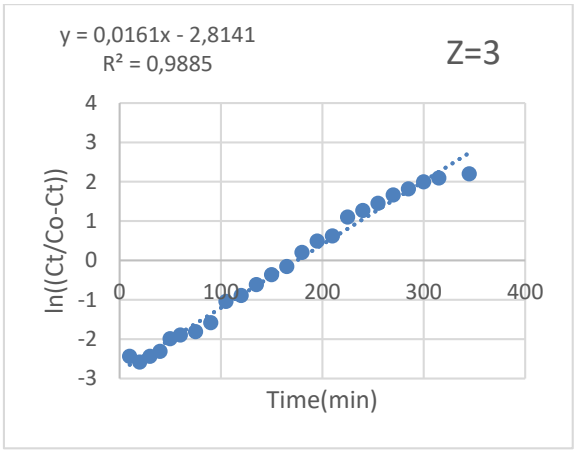


Figure 36: Yoon–Nelson model graph K_{YN} and τ values

K_{YN} = 0.016 (ml min^{-1} g^{-1})

τ = 175.62 (mg g^{-1})

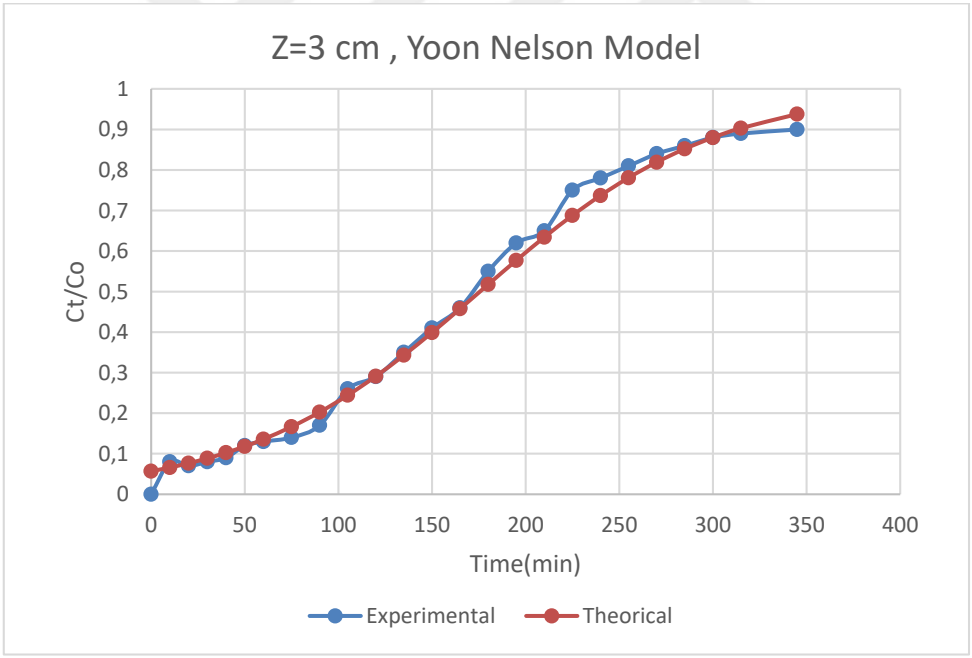


Figure 37: Comparison of experimental value to Theoritical value at

Co=50 ppm, Q=10 ml/min, Z=3 cm Yoon–Nelson model.

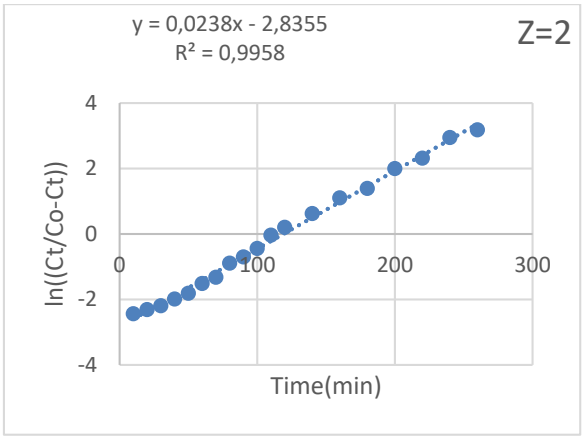


Figure 38: Yoon–Nelson model graph K_{YN} and τ values

K_{YN} = 0.024 (ml min^{-1} g^{-1})

τ = 118.33 (mg g^{-1})

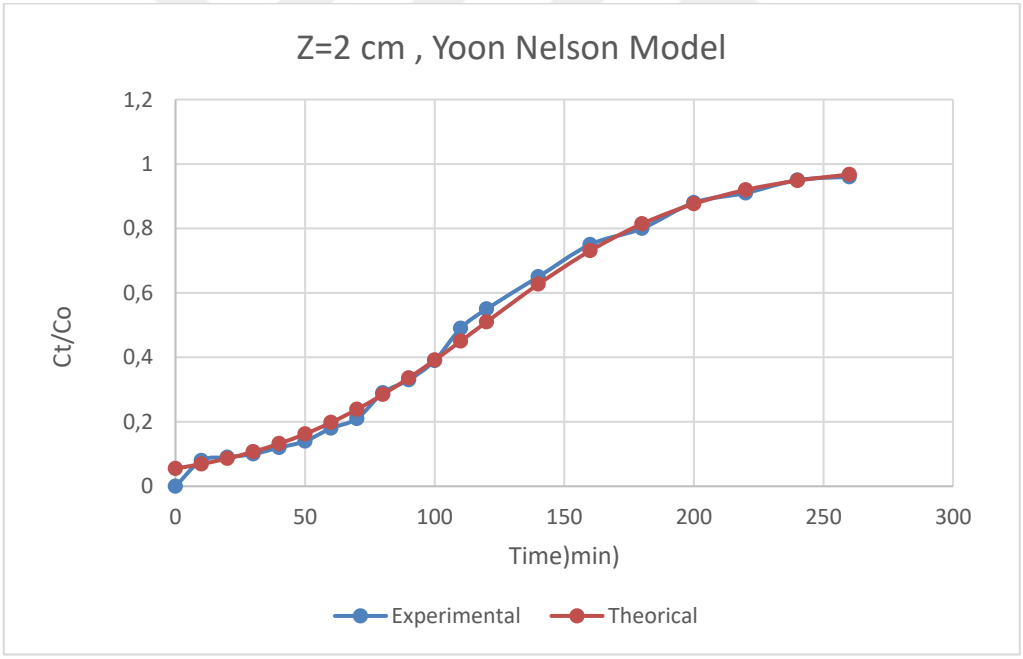


Figure 39: Comparison of experimental value to Theoritical value at

Co=50 ppm, Q=10 ml/min, Z=2 cm Yoon–Nelson model.

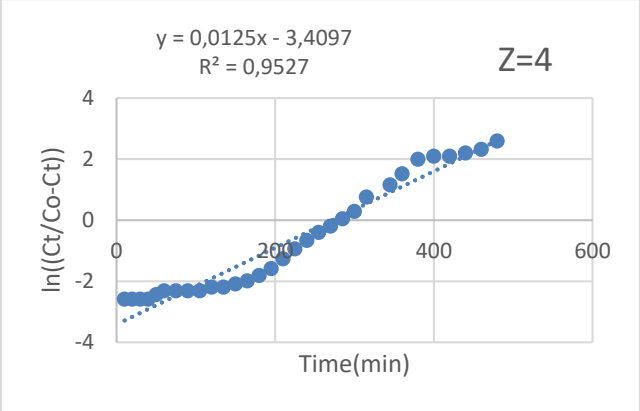


Figure 40: Yoon–Nelson model graph K_{YN} and τ values

K_{YN} = 0.012 (ml min^{-1} g^{-1})

τ = 272.77 (mg g^{-1})

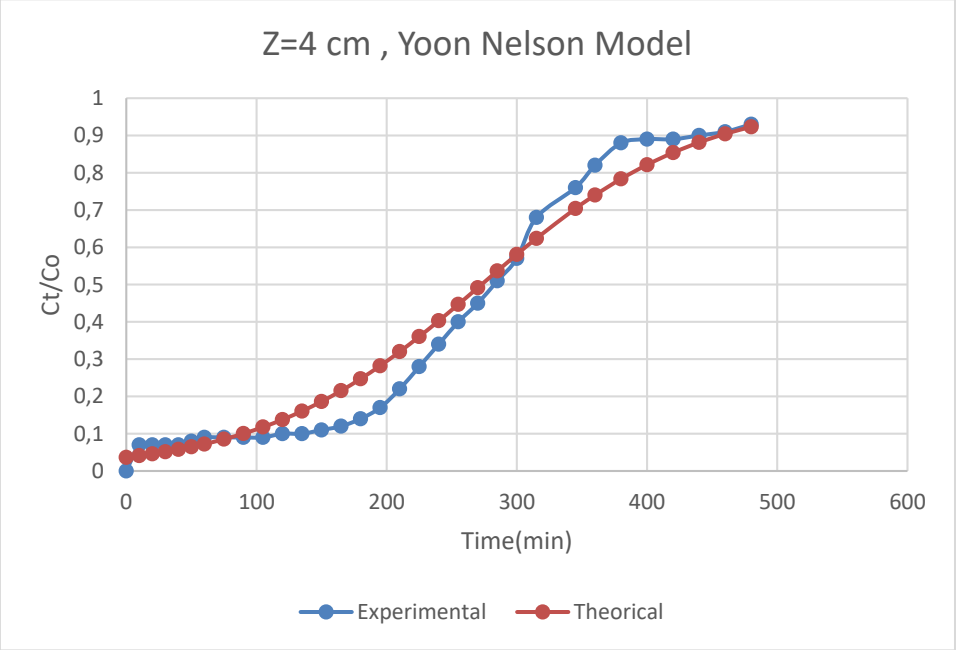


Figure 41: Comparison of experimental value to Theoritical value at

Co=50 ppm, Q=10 ml/min, Z=4 cm Yoon–Nelson model.

Table 2: Yoon–Nelson parameters at different experimental conditions applying nonlinear regression analysis

C_0, (mg/l)	Q, (ml/min)	Z, (cm)	$k_{YN}(x10^{-5})$,l min^{-1} (ml $min^{-1}mg^{-1})10^3$	τ,min	R^2,
50	10	3	16	175	0.99
75	10	3	25	67	0.98
100	10	3	32	45	0.94
75	7.5	3	17	200	0.96
75	12	3	61	38	0.98
50	10	2	24	118	0.99
50	10	4	12	270	0.99

4.2.3 Bed Depth-Time Service (BDST) Model

The adsorption capacity (N_o) and rate constant (K_o) can be determined through the BDST model. From a plot of t versus Z at values of Ct/Co 2, 3 and 4 (figure 42), the correlation constants of BDST according to the a and b of lines are listed in Table 3, respectively. From Table 3, as the value of Ct/Co become higher, the adsorption capacity of the bed No becomes higher too. From the values of R^2, the effectiveness of the BDST model is shown.

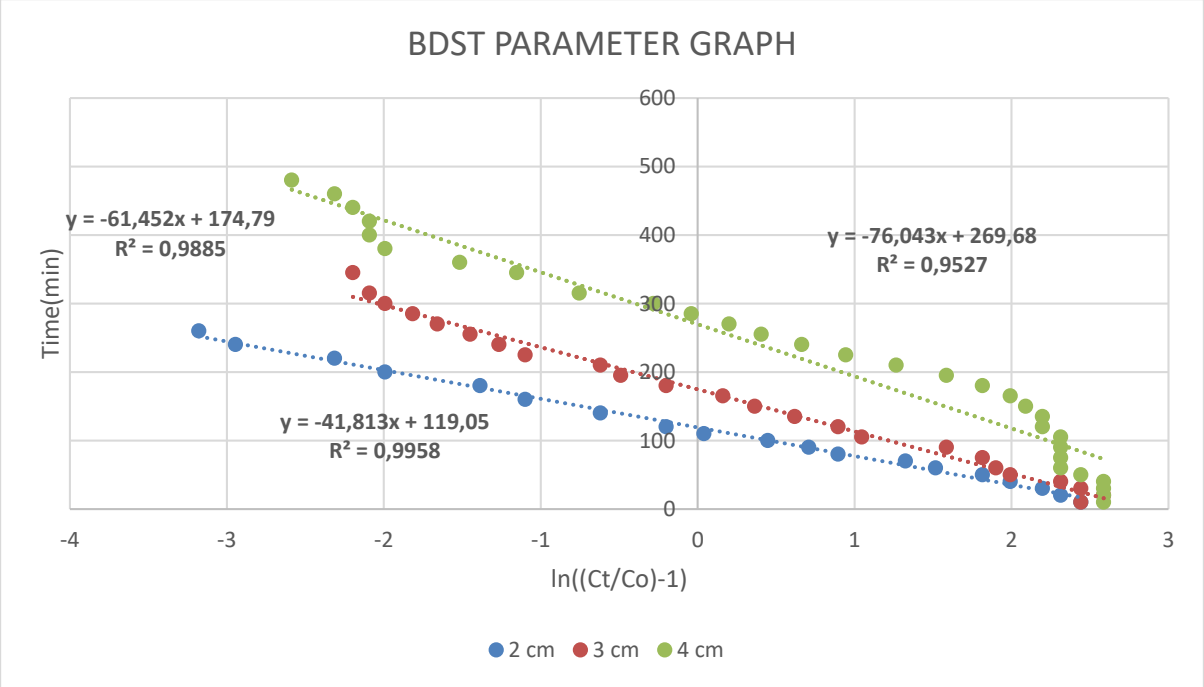


Figure 42: BDST Model Graph K_o and N_o values

a. K_o =0.00026 (l mg^{-1} min^{-1}) at Z=4 cm

N_o = 10733.3 (mg l^{-1})

b. K_o =0.00033 (l mg^{-1} min^{-1}) at Z=3 cm

N_o = 6956.64 (mg l^{-1})

c. K_o =0.00048 (l mg^{-1} min^{-1}) at Z=2 cm

N_o = 10733.3 (mg l^{-1})

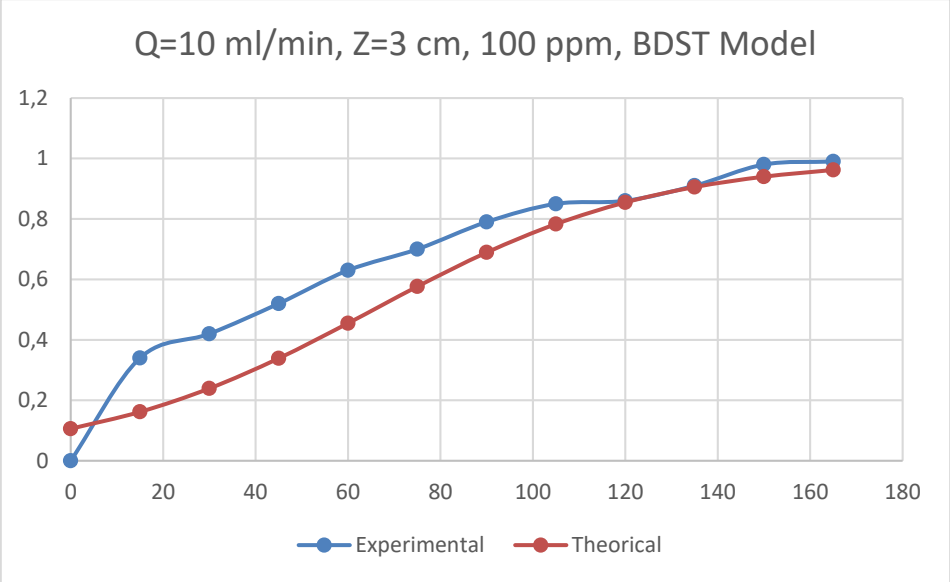


Figure 43: Comparison of experimental value to Theoritical value at

Co=100 ppm, Q=10 ml/min, Z=3 cm BDST model.

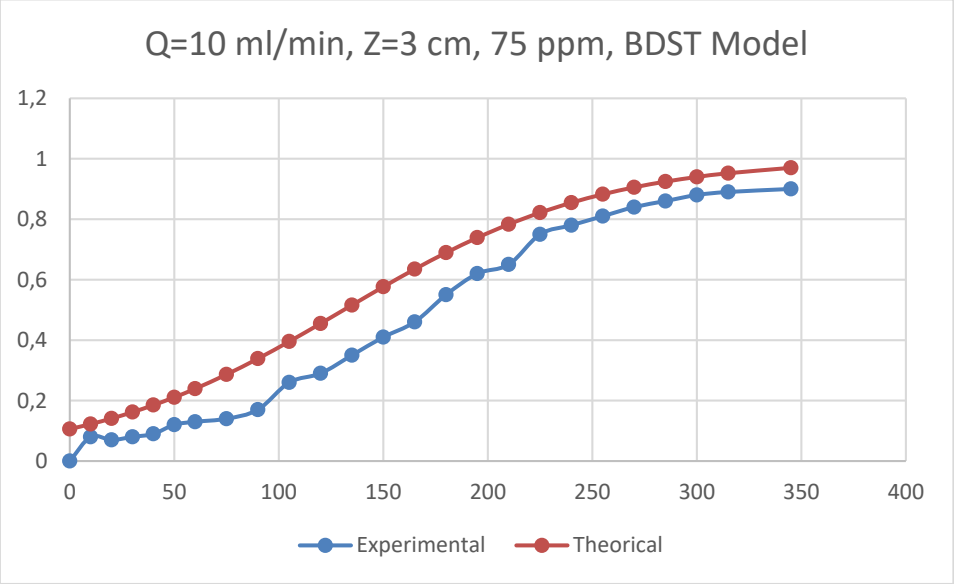


Figure 44: Comparison of experimental value to Theoritical value at

Co=75 ppm, Q=10 ml/min, Z=3 cm BDST model.

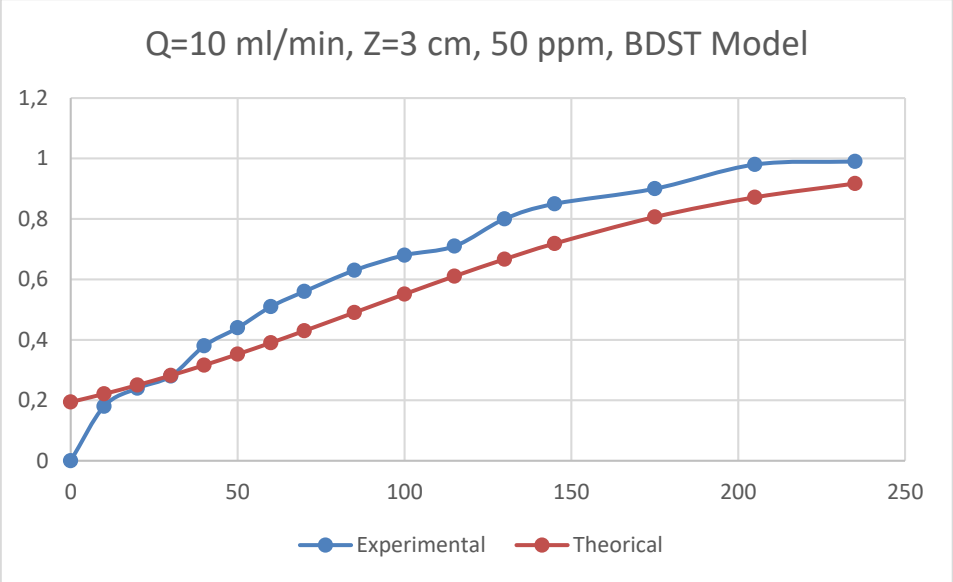


Figure 45: Comparison of experimental value to Theoritical value at

Co=50 ppm, Q=10 ml/min, Z=3 cm BDST model.

Table 3

Calculated constants of the BDST model for the adsorption of MB (C0 = 50 mg l^{-1}, Q = 10 ml min^{-1})

Z cm,	a, min cm^{-1}	b, min	k_o ($x10^{-5}$),l $mg^{-1}min^{-1}$	N_o, ($x10^3$),mg l^{-1}	R^2,
2	-42	119	48	9.476	0.99
3	-61	174	33	6.956	0.98
4	-76	269	26	1.073	0.95

5 CONCLUSION

Considering the experimental results of this investigation, the drawn conclusions are the following:

- Amino functionalized polymers as an adsorbent can be utilized in wastewater treatment to extract Vanadium from solution.
- The adsorption of Vanadium has a correlation with the flow rate, influent Vanadium concentration and bed depth.
- Breakthrough region of the curve were best described by the Thomas model at both experimental and theoretical points and also the working stage or transient stage of the breakthrough curve was shown well by the Thomas model.
- Comparing theoretical curves and experimental data the Thomas model can be utilized to predict the behavior of the adsorption process, while the Yoon–Nelson model cannot do as better prediction.
- The BDST model accurately described the adsorption of Vanadium on Amino functionalized polymers in column mode.

6 REFERENCES

Ambashta, R.D., Sillanpää, M., 2010. Water purification using magnetic assistance: A review. J. Hazard. Mater. https://doi.org/10.1016/j.jhazmat.2010.04.105

Assem, F.L., Oskarsson, A., 2015. Chapter 60 - Vanadium, in: Handbook on the Toxicology of Metals (Fourth Edition). pp. 1347–1367. https://doi.org/http://dx.doi.org/10.1016/B978-0-444-59453-2.00060-3

Blissett, R.S., Rowson, N.A., 2012. A review of the multi-component utilisation of coal fly ash. Fuel. https://doi.org/10.1016/j.fuel.2012.03.024

Bock, E., Smith, N., Rogers, M., Coleman, B., Reiter, M., Benham, B., Easton, Z.M., 2015. Enhanced Nitrate and Phosphate Removal in a Denitrifying Bioreactor with Biochar. J. Environ. Qual. 44, 605. https://doi.org/10.2134/jeq2014.03.0111

Bolan, N.S., Thangarajan, R., Seshadri, B., Jena, U., Das, K.C., Wang, H., Naidu, R., 2013. Landfills as a biorefinery to produce biomass and capture biogas. Bioresour. Technol. https://doi.org/10.1016/j.biortech.2012.08.135

Bratby, J., 2016. Coagulation and Flocculation in Water and Wastewater Treatment. Water 2nd, 538. https://doi.org/10.2166/9781780402321

Chen, D., Zhao, X., Li, F., Zhang, X., 2016. Rejection of nuclides and silicon from boron-containing radioactive waste water using reverse osmosis. Sep. Purif. Technol. 163, 92–99. https://doi.org/10.1016/j.seppur.2016.02.027

Das, T.K., Prusty, S., 2012. Review on Conducting Polymers and Their Applications. Polym. Plast. Technol. Eng. 51, 1487–1500. https://doi.org/10.1080/03602559.2012.710697

Dunn, B., Kamath, H., Tarascon, J.M., 2011. Electrical energy storage for the grid: A battery of choices. Science (80-.). https://doi.org/10.1126/science.1212741

Emik, S., 2014. Preparation and characterization of an IPN type chelating resin containing amino and carboxyl groups for removal of Cu(II) from aqueous solutions. React. Funct. Polym. 75, 63–74. https://doi.org/10.1016/j.reactfunctpolym.2013.12.006

Evans, A., Strezov, V., Evans, T.J., 2012. Assessment of utility energy storage options for increased renewable energy penetration. Renew. Sustain. Energy Rev. https://doi.org/10.1016/j.rser.2012.03.048

Fakhru'l-Razi, A., Pendashteh, A., Abdullah, L.C., Biak, D.R.A., Madaeni, S.S., Abidin, Z.Z., 2009. Review of technologies for oil and gas produced water treatment. J. Hazard. Mater. https://doi.org/10.1016/j.jhazmat.2009.05.044

G. Bohart and E.Q. Adams, Some aspects of the behaviour of charcoal with respect to chlorine, J. Am. Chem. Soc., 42 (1920) 523–544.

Garud, R.M., Kore, S. V, Kore, V.S., Kulkarni, G.S., 2011. A Short Review on Process and Applications of Reverse Osmosis. Univers. J. Environ. Res. Technol. 1, 233–238. https://doi.org/10.1016/j.desal.2010.09.001

Gasik, M.M., 2013. Handbook of ferroalloys, Handbook of Ferroalloys. https://doi.org/10.1016/C2011-0-04204-7

H.C. Thomas, Heterogeneous ion exchange in a flowing system, J. Am. Chem. Soc., 66 (1944) 1664– 1466.

Haibin, L., Zhenling, L., 2010. Recycling utilization patterns of coal mining waste in China. Resour. Conserv. Recycl. 54, 1331–1340. https://doi.org/10.1016/j.resconrec.2010.05.005

Höök, M., Zittel, W., Schindler, J., Aleklett, K., 2010. Global coal production outlooks based on a logistic model. Fuel 89, 3546–3558. https://doi.org/10.1016/j.fuel.2010.06.013

Hosomi, M., 2016. New challenges on wastewater treatment. Clean Technol. Environ. Policy 18, 627–628. https://doi.org/10.1007/s10098-016-1131-1

Hu, Q., Paudyal, H., Zhao, J., Huo, F., Inoue, K., Liu, H., 2014. Adsorptive recovery of vanadium(V) from chromium(VI)-containing effluent by Zr(IV)-loaded orange juice residue. Chem. Eng. J. 248, 79–88. https://doi.org/10.1016/j.cej.2014.03.029

J. Goel, K. Kadirvelu, C. Rajagopal and V.K. Garg, Removal of lead(II) by adsorption using treated granular activated carbon: Batch and column studies, J. Hazard. Mater., 125 (2005) 211–220.

Kajjumba, G.W., Aydın, S., Güneysu, S., 2017. Adsorption isotherms and kinetics of vanadium by shale and coal waste. Adsorpt. Sci. Technol. https://doi.org/10.1177/0263617417733586

Kurniawan, T.A., Chan, G.Y.S., Lo, W.H., Babel, S., 2006. Physico-chemical treatment techniques for wastewater laden with heavy metals. Chem. Eng. J. 118, 83–98. https://doi.org/10.1016/j.cej.2006.01.015

Mazed, M.A., Mazed, S., 2010. Nutritional supplement for the prevention of cardiovascular disease, Alzheimer's disease, diabetes, and regulation and reduction of blood sugar and insulin resistance. U.S. Pat. Appl. Publ.

Mohan, S., Gandhimathi, R., 2009. Removal of heavy metal ions from municipal solid waste leachate using coal fly ash as an adsorbent. J. Hazard. Mater. 169, 351–359. https://doi.org/10.1016/j.jhazmat.2009.03.104

Mthombeni, N.H., Mbakop, S., Ochieng, A., Onyango, M.S., 2016. Vanadium (V) adsorption isotherms and kinetics using polypyrrole coated magnetized natural zeolite. J. Taiwan Inst. Chem. Eng. 66, 172–180. https://doi.org/10.1016/j.jtice.2016.06.016

Narayanan, K.B., Sakthivel, N., 2010. Biological synthesis of metal nanoparticles by microbes. Adv. Colloid Interface Sci. https://doi.org/10.1016/j.cis.2010.02.001

Nataraj, S.K., Hosamani, K.M., Aminabhavi, T.M., 2006. Distillery wastewater treatment by the membrane-based nanofiltration and reverse osmosis processes. Water Res. 40, 2349–2356. https://doi.org/10.1016/j.watres.2006.04.022

Ortega-Bravo, J.C., Ruiz-Filippi, G., Donoso-Bravo, A., Reyes-Caniupán, I.E., Jeison, D., 2016. Forward osmosis: Evaluation thin-film-composite membrane for municipal sewage concentration. Chem. Eng. J. 306, 531–537. https://doi.org/10.1016/j.cej.2016.07.085

Paraskeva, P., Diamadopoulos, E., 2006. Technologies for olive mill wastewater (OMW) treatment: A review. J. Chem. Technol. Biotechnol. https://doi.org/10.1002/jctb.1553

R.M. Clark, Evaluating the cost and performance of field-scale granular activated carbon systems, Environ. Sci, Technol., 21 (1987) 573–580.

R.P. Han, J.H. Zhang, W.H. Zou, H.J. Xiao, J. Shi and H.M. Liu, Biosorption of copper(II) and lead(II) from aqueous solution by chaff in a fixed-bed column, J. Hazard. Mater., 133 (2006) 262–268.

Rauf, M.A., Meetani, M.A., Hisaindee, S., 2011. An overview on the photocatalytic degradation of azo dyes in the presence of TiO2 doped with selective transition metals. Desalination. https://doi.org/10.1016/j.desal.2011.03.071

Ribeiro, J., Flores, D., Ward, C.R., Silva, L.F.O., 2010. Identification of nanominerals and nnoparticles in burning coal waste piles from Portugal. Sci. Total Environ. 408, 6032–6041. https://doi.org/10.1016/j.scitotenv.2010.08.046

Serkan Emik 2014. Preparation and characterization of an IPN type chelating resin containing amino and carboxyl groups for removal of Cu(II) from aqueous solutions. Reactive & Functional Polymers 75, 63–74. https://doi.org/10.1016/j.reactfunctpolym.2013.12.006

Smolders, A.J.P., Lucassen, E.C.H.E.T., Bobbink, R., Roelofs, J.G.M., Lamers, L.P.M., 2010. How nitrate leaching from agricultural lands provokes phosphate eutrophication in groundwater fed wetlands: The sulphur bridge. Biogeochemistry 98, 1–7. https://doi.org/10.1007/s10533-009-9387-8

Song, Y., Dong, B., Gao, N., Deng, Y., 2015. Comparative evaluation of aluminum sulfate and ferric sulfate-induced coagulations as pretreatment of microfiltration for treatment of surface water. Int. J. Environ. Res. Public Health 12, 6700–6709. https://doi.org/10.3390/ijerph120606700

Suckeveriene, R.Y., Zelikman, E., Mechrez, G., Narkis, M., 2011. Literature review: Conducting carbon nanotube/polyaniline nanocomposites. Rev. Chem. Eng. https://doi.org/10.1515/REVCE.2011.004

Türgay, O., Ersöz, G., Atalay, S., Forss, J., Welander, U., 2011. The treatment of azo dyes found in textile industry wastewater by anaerobic biological method and chemical oxidation. Sep. Purif. Technol. 79, 26–33. https://doi.org/10.1016/j.seppur.2011.03.007

United Nations, 2016. 2014 Energy Statistics Yearbook.

Y.H. Yoon and J.H. Nelson, Aplication of gas adsorption kinetics. I. A theoretical model for respirator cartridge service time, Am. Ind. Hyg. Assoc. J., 45 (1984) 509–516.

Zhang, Y.M., Bao, S.X., Liu, T., Chen, T.J., Huang, J., 2011. The technology of extracting vanadium from stone coal in China: History, current status and future prospects. Hydrometallurgy 109, 116–124. https://doi.org/10.1016/j.hydromet.2011.06.002

Z. Zulfadhly, M.D. Mashitah and S. Bhatia, Heavy metals removal in fixed-bed column by

the macro fungus Pycnoporus sanguineus, Environ. Pollut., 112 (2001) 463–470.

Z. Aksu and F. Gonen, Biosorption of phenol by immobilized activated sludge in a continuous packed bed: prediction of breakthrough curves, Process Biochem., 39 (2004) 599–613.

7 APPENDICES

7.1 Appendix 1: Experimental data first group of experiments effect of concentration on the breakthrough curve

At Co = 100 ppm; Q = 10 ml/min; Z = 3 cm

Ct/Co (Co=100)	
t	Ct/Co
15	34
30	42
45	52
60	63
75	70
90	79
105	85
120	86
135	91
150	98
165	100

At Co = 50 ppm; Q = 10 ml/min; Z = 3 cm

Ct/Co (Co=50)	
t	Ct/Co
10	4
20	4
30	4
40	5
50	6
60	7
75	7
90	9
105	13
120	15
135	18
150	21
165	23
180	28
195	31
210	33
225	38
240	39
255	41
270	42
285	43
300	44
315	45
345	45

At Co = 75 ppm; Q = 10 ml/min; Z = 3 cm

Ct/Co (Co=75)	
t	Ct/Co
10	13,50
20	18,00
30	21,00
40	28,50
50	33,00
60	38,25
70	42,00
85	47,25
100	51,00
115	53,25
130	60,00
145	63,75
175	67,50
205	73,50
235	74,25

Comparison between experimental data and Thomas model data

	Theorical Ct/C0 according to Thomas Model							
		Co=100		**Co=50**			**Co=75**	
t	**Theo.**	**Exp.**	**t**	**Theo.**	**Exp.**	**t**	**Theo.**	**Exp.**
0		**0**	**0**		**0**	0		0
15	0,2770	0,340000	10	0,032868	0,04	10	0,180771	0,135
30	0,3824	0,420000	20	0,038136	0,035	20	0,206776	0,18
45	0,5001	0,520000	30	0,044169	0,04	30	0,235448	0,21
60	0,6179	0,630000	40	0,05105	0,045	40	0,266758	0,285
75	0,7232	0,700000	50	0,058865	0,06	50	0,300595	0,33
90	0,8085	0,790000	60	0,067696	0,065	60	0,336752	0,3825
105	0,8722	0,850000	75	0,08301	0,07	70	0,374928	0,42
120	0,9169	0,860000	90	0,100979	0,085	85	0,435085	0,4725
135	0,9469	0,910000	105	0,121703	0,13	100	0,497217	0,51
150	0,9665	0,980000	120	0,145132	0,145	115	0,559434	0,5325
165	0,9790	0,990000	135	0,171033	0,175	130	0,619839	0,6
			150	0,198965	0,205	145	0,676748	0,6375
			165	0,228292	0,23	175	0,775367	0,675
			180	0,258235	0,275	205	0,850543	0,735
			195	0,287942	0,31	235	0,903686	0,7425
			210	0,316592	0,325			
			225	0,343475	0,375			
			240	0,36806	0,39			
			255	0,39002	0,405			
			270	0,409226	0,42			
			285	0,425717	0,43			
			300	0,439654	0,44			
			315	0,451276	0,445			
			345	0,468687	0,45			

Comparison between experimental data and Yoon-Nelson model data

	Exp.	Theo		Exp.	Theo.		Exp.	Theo.
Co = 100			Co = 50			Co = 75		
0	0	0,19378	0	0	0,056567	0	0	0,157095
15	0,34	0,279764	10	0,08	0,065737	10	0,18	0,193099
30	0,42	0,385651	20	0,07	0,076273	20	0,24	0,235052
45	0,52	0,503592	30	0,08	0,088338	30	0,28	0,282925
60	0,63	0,621135	40	0,09	0,102101	40	0,38	0,336261
75	0,7	0,725989	50	0,12	0,117731	50	0,44	0,394126
90	0,79	0,81067	60	0,13	0,135393	60	0,51	0,455121
105	0,85	0,873732	75	0,14	0,166021	70	0,56	0,517493
120	0,86	0,917916	90	0,17	0,201959	85	0,63	0,60945
135	0,91	0,947567	105	0,26	0,243406	100	0,68	0,694236
150	0,98	0,966894	120	0,29	0,290265	115	0,71	0,767634
165	0,99	0,979253	135	0,35	0,342067	130	0,8	0,827784
			150	0,41	0,39793	145	0,85	0,8749
			165	0,46	0,456586	175	0,9	0,936731
			180	0,55	0,51647	205	0,98	0,969082
			195	0,62	0,575885	235	0,99	0,985153
			210	0,65	0,633185			
			225	0,75	0,686951			
			240	0,78	0,736121			
			255	0,81	0,780041			
			270	0,84	0,818453			
			285	0,86	0,851435			
			300	0,88	0,879309			
			315	0,89	0,902552			
			345	0,9	0,937374			

7.2 Appendix 2: Experimental data second group of experiments effect of the flow rate on the breakthrough curve

At Co = 100 ppm; Q = 7.5 ml/min; Z = 3 cm

Ct/Co at Q=7.5ml/min	
t	Ct/Co
10	3
20	3,75
30	3,75
40	4,5
50	6
60	7,5
70	9
80	11,25
90	13,5
100	15
110	16,5
120	18,75
130	19,5
145	21,75
160	24
175	27,75
190	31,5
205	34,5
220	39,75
235	42,75

250	47,25
265	52,5
280	57
295	62,25
305	68,25
335	73,5
365	72,75

At Co = 100 ppm; Q = 10 ml/min; Z = 3 cm

Ct/Co at Q=10ml/min	
t	Ct/Co
10	13,50
20	18,00
30	21,00
40	28,50
50	33,00
60	38,25
70	42,00
85	47,25
100	51,00
115	53,25
130	60,00
145	63,75
175	67,50
205	73,50
235	74,25

At Co = 100 ppm; Q = 12.5 ml/min; Z = 3 cm

Ct/Co at Q=12.5ml/min	
t	Ct/Co
10	11,25
20	19,5
30	30,75
40	39
50	48
60	58,5
70	63
80	70,5
90	73,5
100	73,5
110	73,5

Comparison between experimental data and Thomas model data

	Theorical Ct/C0 according to Thomas Model							
		Q=7.5		Q=10			Q=12.5	
t	Theo.	Exp.	t	Theo.	Exp.	t	Theo.	Exp.
0		0	0		0	0		0
10	0,028973	0,03	10	0,180771	0,135	10	0,11633	0,1125
20	0,034425	0,0375	20	0,206776	0,18	20	0,189761	0,195
30	0,040845	0,0375	30	0,235448	0,21	30	0,288444	0,3075
40	0,04838	0,045	40	0,266758	0,285	40	0,401655	0,39
50	0,057194	0,06	50	0,300595	0,33	50	0,510184	0,48
60	0,067459	0,075	60	0,336752	0,3825	60	0,59772	0,585
70	0,079356	0,09	70	0,374928	0,42	70	0,659003	0,63
80	0,093064	0,1125	85	0,435085	0,4725	80	0,697778	0,705
90	0,108756	0,135	100	0,497217	0,51	90	0,720764	0,735
100	0,126585	0,15	115	0,559434	0,5325	100	0,733866	0,735
110	0,146668	0,165	130	0,619839	0,6	110	0,741168	0,735
120	0,169072	0,1875	145	0,676748	0,6375			
130	0,1938	0,195	175	0,775367	0,675			
145	0,235045	0,2175	205	0,850543	0,735			
160	0,28064	0,24	235	0,903686	0,7425			
175	0,32942	0,2775						
190	0,379818	0,315						
205	0,430043	0,345						
220	0,478328	0,3975						
235	0,523169	0,4275						
250	0,563495	0,4725						
265	0,598725	0,525						
280	0,628732	0,57						
295	0,653744	0,6225						
305	0,667863	0,6825						
335	0,699843	0,735						
365	0,719932	0,7275						

Comparison between experimental data and Yoon-Nelson model data

	Exp.	Theo		Exp.	Theo.		Exp.	Theo.
Q = 7.5 ml/min			Q = 10 ml/min			Q = 12.5 ml/min		
0	0	0,032483	0	0	0,157095	0	0	0,090545
10	0,04	0,038272	10	0,18	0,193099	10	0,15	0,154857
20	0,05	0,045045	20	0,24	0,235052	20	0,26	0,252183
30	0,05	0,05295	30	0,28	0,282925	30	0,41	0,38296
40	0,06	0,062152	40	0,38	0,336261	40	0,52	0,533201
50	0,08	0,072831	50	0,44	0,394126	50	0,64	0,677651
60	0,1	0,085177	60	0,51	0,455121	60	0,78	0,794619
70	0,12	0,099392	70	0,56	0,517493	70	0,84	0,876857
80	0,15	0,115679	85	0,63	0,60945	80	0,94	0,929103
90	0,18	0,134237	100	0,68	0,694236	90	0,98	0,960189
100	0,2	0,15525	115	0,71	0,767634	100	0,98	0,977968
110	0,22	0,178873	130	0,8	0,827784	110	0,98	0,987907
120	0,25	0,205217	145	0,85	0,8749			
130	0,26	0,234334	175	0,9	0,936731			
145	0,29	0,283127	205	0,98	0,969082			
160	0,32	0,337602	235	0,99	0,985153			
175	0,37	0,396756						
190	0,42	0,459091						
205	0,46	0,522734						
220	0,53	0,585647						
235	0,57	0,645885						
250	0,63	0,701824						
265	0,7	0,752315						
280	0,76	0,796733						
295	0,83	0,834933						
305	0,91	0,85705						
335	0,98	0,90896						
365	0,97	0,943267						

7.3 Appendix 3: Experimental data third group of experiments effect of different bed depth on the breakthrough curve

At Co = 100 ppm; Q = 7.5 ml/min; Z = 3 cm

Ct/Co at Z=3cm	
t	**Ct/Co**
0	0
10	4,000
20	3,500
30	4,000
40	4,500
50	6,000
60	6,500
75	7,000
90	8,500
105	13,000
120	14,500
135	17,500
150	20,500
165	23,000
180	27,500
195	31,000
210	32,500
225	37,500
240	39,000
255	40,500
270	42,000
285	43,000
300	44,000
315	44,500
345	45,000

At Co = 100 ppm; Q = 7.5 ml/min; Z = 2 cm

Ct/Co at Z=2cm	
t	**Ct/Co**
0	0
10	4,000
20	4,500
30	5,000
40	6,000
50	7,000
60	9,000
70	10,500
80	14,500
90	16,500
100	19,500
110	24,500
120	27,500
140	32,500
160	37,500
180	40,000
200	44,000
220	45,500
240	47,500
260	48,000

At Co = 100 ppm; Q = 7.5 ml/min; Z = 4 cm

Ct/Co at Z=4cm	
t	**Ct/Co**
10	3,008005565
20	3,334445198

30	3,693526757
40	4,087889896
50	4,520249465
60	4,993364515
75	5,785489779
90	6,684610752
105	7,69913207
120	8,8362168
135	10,10113567
150	11,49655759
165	13,02183538
180	14,67236216
195	16,43908958
210	18,30830357
225	20,26174065
240	22,27709434
255	24,32891126
270	26,38981558
285	28,43194436
300	30,42843755
315	32,35481604
345	35,91758346
360,00	37,52518036
380,00	39,46989557
400,00	41,18268138
420,00	42,66862006
440,00	43,94098373
460,00	45,01830953
480,00	45,92185905

Comparison between experimental data and Thomas model data

	Theorical Ct/C0 according to Thomas Model							
		Z=3		**Z=2**			**Z=4**	
t	**Ct/Co**	**Exp. Ct/Co**	**t**	**Ct/Co**	**exp. Ct/Co**	**t**	**Ct/Co**	**exp. Ct/Co**
0		**0**	**0**		**0**	**0**		**0**
10	0,045182	0,04	10	0,049864	0,04	10	0,033679	0,03008
20	0,051275	0,035	20	0,060116	0,045	20	0,037303	0,033344
30	0,058086	0,04	30	0,072137	0,05	30	0,041282	0,036935
40	0,065668	0,045	40	0,086091	0,06	40	0,045644	0,040879
50	0,074074	0,06	50	0,1021	0,07	50	0,050417	0,045202
60	0,08335	0,065	60	0,120222	0,09	60	0,055627	0,049934
75	0,098972	0,07	70	0,140426	0,105	75	0,064322	0,057855
90	0,116701	0,085	80	0,162571	0,145	90	0,07415	0,066846
105	0,136525	0,13	90	0,186398	0,165	105	0,085186	0,076991
120	0,158326	0,145	100	0,211528	0,195	120	0,097488	0,088362
135	0,181866	0,175	110	0,23748	0,245	135	0,111091	0,101011
150	0,206788	0,205	120	0,263706	0,275	150	0,125998	0,114966
165	0,232628	0,23	140	0,314713	0,325	165	0,142174	0,130218
180	0,258846	0,275	160	0,360533	0,375	180	0,15954	0,146724
195	0,284871	0,31	180	0,398671	0,4	195	0,177973	0,164391
210	0,310147	0,325	200	0,428449	0,44	210	0,197302	0,183083
225	0,334183	0,375	220	0,450561	0,455	225	0,217313	0,202617
240	0,356582	0,39	240	0,466376	0,475	240	0,23776	0,222771
255	0,377069	0,405	260	0,477386	0,48	255	0,258372	0,243289
270	0,395486	0,42				270	0,278871	0,263898
285	0,41179	0,43				285	0,298983	0,284319
300	0,426027	0,44				300	0,318458	0,304284
315	0,43831	0,445				315	0,337073	0,323548
345	0,457676	0,45				345	0,371058	0,359176
						360	0,386208	0,375252
						380	0,404382	0,394699
						400	0,420253	0,411827
						420	0,43392	0,426686
						440	0,445549	0,43941
						460	0,455341	0,450183
						480	0,463517	0,459219

Comparison between experimental data and Yoon-Nelson model data

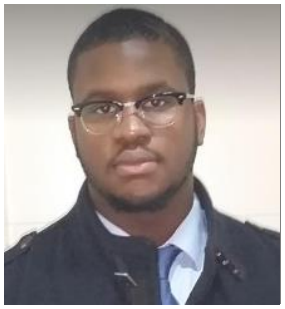
Exp.	Theo	Exp.	Theo.	Exp.	Theo.	
Z= 3 cm		Z= 2 cm		Z= 4 cm		
0	0,056786	0	0,055201	0	0,036498	
0,08	0,065989	0,08	0,069139	0,07	0,040961	
0,07	0,076562	0,09	0,086275	0,07	0,045943	
0,08	0,088669	0,1	0,107169	0,07	0,051499	
0,09	0,102477	0,12	0,13239	0,07	0,057687	
0,12	0,118157	0,14	0,162466	0,08	0,064567	
0,13	0,135873	0,18	0,197817	0,09	0,072204	
0,14	0,166589	0,21	0,238669	0,09	0,085231	
0,17	0,20262	0,29	0,28496	0,09	0,100353	
0,26	0,244161	0,33	0,336263	0,09	0,117812	
0,29	0,29111	0,39	0,391743	0,1	0,137844	
0,35	0,34299	0,49	0,450168	0,1	0,160662	
0,41	0,398912	0,55	0,510001	0,11	0,18644	
0,46	0,457602	0,65	0,62715	0,12	0,215293	
0,55	0,517493	0,75	0,73106	0,14	0,247254	
0,62	0,576885	0,8	0,814574	0,17	0,282253	
0,65	0,634136	0,88	0,876534	0,22	0,3201	
0,75	0,687831	0,91	0,919828	0,28	0,360473	
0,78	0,736916	0,95	0,948827	0,34	0,40292	
0,81	0,780743	0,96	0,967705	0,4	0,446873	
0,84	0,819061			0,45	0,491673	
0,86	0,851953			0,51	0,536606	
0,88	0,879743			0,57	0,580953	
0,89	0,902911			0,68	0,62403	
0,9	0,937614			0,76	0,704056	
				0,82	0,740138	
				0,88	0,783586	
				0,89	0,821521	
				0,89	0,854045	
				0,9	0,881497	
				0,91	0,904364	
				0,93	0,923203	

Comparison between experimental data and BDST model data

BSDT Model								
Q=10, Z=3 , Co=100			Q=10, Z=3 , Co=75			Q=10, Z=3 , Co=50		
t	Exp	Theo	t	Exp	Theo	t	Exp	Theo
0	0	0,105952	0	0	0,105952	0	0	0,194372
15	0,34	0,161842	10	0,08	0,122384	10	0,18	0,221125
30	0,42	0,239322	20	0,07	0,140963	20	0,24	0,250417
45	0,52	0,338897	30	0,08	0,161842	30	0,28	0,282182
60	0,63	0,455114	40	0,09	0,185147	40	0,38	0,316277
75	0,7	0,576435	50	0,12	0,210963	50	0,44	0,352469
90	0,79	0,689192	60	0,13	0,239322	60	0,51	0,390437
105	0,85	0,78322	75	0,14	0,286528	70	0,56	0,42978
120	0,86	0,854795	90	0,17	0,338897	85	0,63	0,490337
135	0,91	0,905587	105	0,26	0,395531	100	0,68	0,55118
150	0,98	0,939862	120	0,29	0,455114	115	0,71	0,610528
165	0,99	0,962213	135	0,35	0,516011	130	0,8	0,666773
			150	0,41	0,576435	145	0,85	0,718638
			165	0,46	0,634657	175	0,9	0,806262
			180	0,55	0,689192	205	0,98	0,871478
			195	0,62	0,738934	235	0,99	0,917001
			210	0,65	0,78322			
			225	0,75	0,821805			
			240	0,78	0,854795			
			255	0,81	0,882551			
			270	0,84	0,905587			
			285	0,86	0,924491			
			300	0,88	0,939862			
			315	0,89	0,952265			
			345	0,9	0,970153			

CURRICULUM VITAE

Personal Information	
Name Surname	Abdoulaye Mamadou TRAORE
Place of Birth	Bamako, Mali
Date of Birth	16.08 1993
Nationality	❒ T.C. ☑ Other:
Phone Number	00905373933041
Email	Amtraore93@gmail.com
Web Page	



Educational Information	
B. Sc.	
University	Fatih University
Faculty	Engineering
Department	Genetics and Bioengineering
Graduation Year	30.07.2015

M. Sc.	
University	Istanbul University-Cerrahpasa
Institute	Institute of Graduate Studies
Department	Department of Environmental Engineering
Programme	Environmental Engineering Programme

Ph. D.	
University	
Institute	
Department	
Programme	

Publications